

PhotoFramer: Multi-modal Image Composition Instruction

Zhiyuan You¹², Ke Wang³, He Zhang⁴, Xin Cai², Jinjin Gu⁵,
Tianfan Xue²⁶⁷, Chao Dong¹⁶⁸, Zhoutong Zhang³

¹Shenzhen Institutes of Advanced Technology, Chinese Academy of Sciences

²Multimedia Laboratory, The Chinese University of Hong Kong

³Adobe NextCam ⁴Adobe Research ⁵INSAIT, Sofia University “St. Kliment Ohridski”

⁶Shanghai AI Laboratory ⁷CPII under InnoHK ⁸Shenzhen University of Advanced Technology

zhiyuanyou@foxmail.com, tfxue@ie.cuhk.edu.hk, chao.dong@siat.ac.cn, zhoutongz@adobe.com

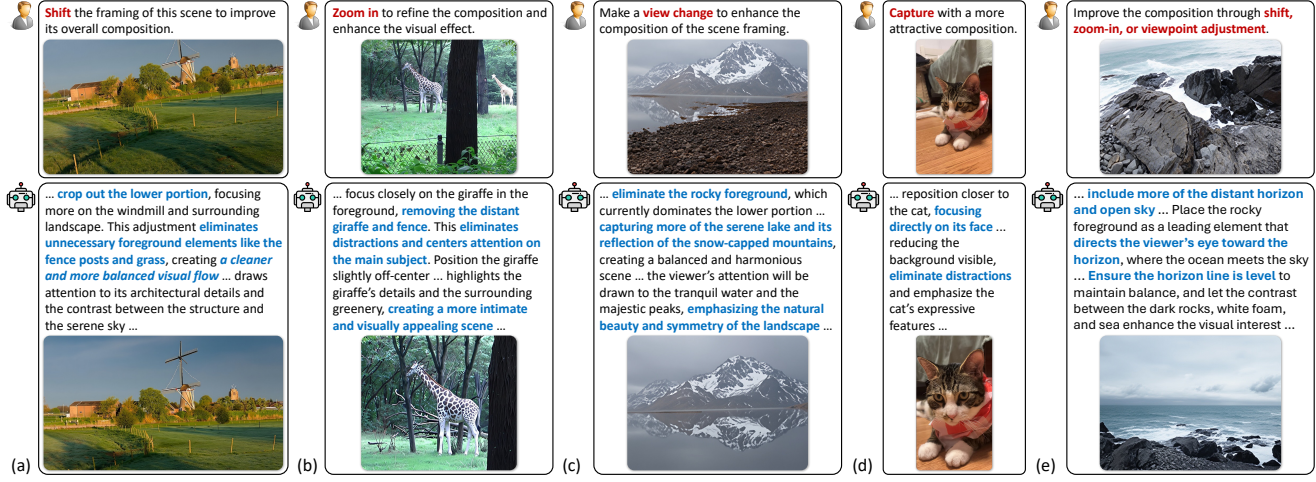


Figure 1. We propose PhotoFramer, a model designed for composition instruction during photo capturing. Given a poorly composed image, PhotoFramer first describes how to improve the composition in natural language and then generates an example image that follows the described suggestions. The photo-taker can follow the textual guidance and the example image to capture a better-composed photo.

Abstract

Composition matters during the photo-taking process, yet many casual users struggle to frame well-composed images. To provide effective composition guidance, we introduce PhotoFramer, a multi-modal composition instruction framework. Given a poorly composed image, PhotoFramer first describes how to improve the composition in natural language and then generates a well-composed example image. To train such a model, we curate a large-scale dataset. Inspired by how humans take photos, we organize composition guidance into a hierarchy of sub-tasks: shift, zoom-in, and view-change tasks. Shift and zoom-in data are sampled from existing cropping datasets, while view-change data are obtained via a two-stage pipeline. First, we sample pairs with varying viewpoints from multi-view datasets, and train a degradation model to transform well-composed photos into poorly composed ones. Second, we apply this degradation model to expert-taken photos to synthesize poor images

to form training pairs. Using this dataset, we finetune a model that jointly processes and generates both text and images, enabling actionable textual guidance with illustrative examples. Extensive experiments demonstrate that textual instructions effectively steer image composition, and coupling them with exemplars yields consistent improvements over exemplar-only baselines. PhotoFramer offers a practical step toward composition assistants that make expert photographic priors accessible to everyday users. Codes, model weights, and datasets have been released in <https://zhiyuanyou.github.io/photoframer>.

1. Introduction

Modern mobile cameras have become increasingly powerful [7, 18, 37, 50]. Equipped with these cameras, the users could capture high-resolution, noise-free, and well-exposed photos. However, many casual users still struggle to capture visually pleasing photos. As shown in the top images of Fig. 1, these photos appear visually unappealing due to their

poor composition. For instance, in Fig. 1e, the sea horizon is tilted relative to the image border, and the foreground rocks dominate the frame excessively. Therefore, providing amateur photographers with composition guidance during photo capturing is of great importance [12, 29, 71].

Casual users can be guided more effectively through a combination of textual and visual instructions. Consider a captured farm scene in Fig. 1a, textual instruction “eliminates the fence posts and grass” provides concrete and actionable operations, along with detailed reasons (*e.g.*, “creating a cleaner and more balanced visual flow”). Meanwhile, in the bottom of Fig. 1a, the well-composed example photo capturing the same farm scene is intuitive and easy to follow, consistent with prior findings [12, 74].

To leverage the strengths of both modalities, we introduce PhotoFramer, a multi-modal image composition instruction framework that provides detailed textual guidance paired with corresponding visual example photos.

To build this composition instruction model, we design a hierarchical set of tasks inspired by how humans take photos. Humans typically first determine a suitable position and angle (*i.e.*, vantage point), choose an appropriate focal length, and then finetune subject placement and alignment [13, 24]. Accordingly, PhotoFramer consists of three sub-tasks: view-change (Fig. 1c), zoom-in (Fig. 1b), and shift (Fig. 1a) tasks. In addition, when the user does not specify a task type (as in Fig. 1de), PhotoFramer automatically determines suitable operations. We show that the model does not merely select one task type, but adaptively fuses multiple operations to achieve better composition.

Under this task formulation, we construct a comprehensive multi-modal dataset containing “poor image, good image, text guidance” triplets. For the shift and zoom-in sub-tasks, we sample image pairs from existing cropping datasets [5, 56, 63, 64, 70]. For the view-change sub-task, we first sample image pairs with different viewpoints from multi-view datasets [32], and then train a degradation model that converts well-composed photos into compositionally degraded ones. We then apply this model to expert-taken photos [9] to synthesize view-change examples. Finally, we employ the vision-language model Qwen2.5-VL-32B [1] to annotate text guidance for each pair. In total, we collect 207K triplets, serving as the foundation for model training.

Equipped with the above dataset, we finetune the unified understanding-generation model [8, 14, 49, 60, 62] to generate both textual guidance and example image. As depicted in Fig. 1, our model is required to process inputs and outputs that include both texts and images. Consequently, vision-language models [1, 35, 76] that can only produce textual outputs, as well as image generation or editing models [2, 3, 45] that can only produce images, are unsuitable. We therefore employ the unified understanding-generation model Bagel [8] as our base and fine-tune it using our pro-

posed dataset. Experiments show that textual guidance effectively guides image generation, highlighting the advantages of the text-vision joint modeling framework.

Extensive comparisons and ablations further confirm the superiority of our PhotoFramer over baselines. We hope this work serves as a stepping stone toward composition assistants that help everyday users capture expert-level photos.

2. Related Works

Composition understanding is the foundation for composition instruction. Composition classification [25, 71, 75] defines multiple composition categories (*e.g.*, rule-of-thirds, symmetrical, *etc.*). Some works [69–71] focus on score-based composition assessment. Recent works [4, 33] utilize powerful vision language models [1, 39, 77] to build multi-aspect aesthetics (*i.e.*, including composition) assessment models with joint scoring and descriptive outputs.

Image cropping is a common approach to enhance the composition. Given an original image, this task aims to find a cropped patch with better composition. Extensive cropping datasets can be broadly categorized into two types. The first type is densely annotated, where multiple crops are labeled per image [47, 56, 64, 69, 70]. The second type is sparsely annotated, where only the best crop is labeled per image [5, 10, 63]. Built upon these datasets, deep learning models have achieved substantial progress. Many methods [10, 20, 28, 47, 53, 55, 56, 63, 64, 69, 70, 72] adopt a two-stage strategy: first generating crop candidates, then selecting the optimal one. Other coordinate regression methods [6, 15, 16, 26, 27, 36] directly predict crop boundaries. Recently, GenCrop [17] leverages Stable Diffusion [45] to outpaint professional photos for dataset expansion. ProCrop [73] retrieves compositionally similar reference images to guide the cropping process. However, image cropping remains a post-processing operation applied after photo capture. In contrast, our work aims to guide users *during* the capturing process to take well-composed photos.

Composition guidance. Traditional methods rely on retrieval to search similar images in the database as user reference [11, 12, 74]. However, retrieval-based guidance suffers from scene and subject mismatch, making it hard to follow. Recent CPAM [29] could automatically provide photographers with camera pose adjustment guidance. Our work differs from CPAM in three key aspects. First, CPAM predicts only adjusted yaw and pitch angles, while we generate both text instruction and a good example image, offering a more intuitive and informative guide. Second, CPAM is limited to yaw and pitch adjustments, whereas our model additionally supports zoom control and large-scale viewpoint changes. Third, CPAM employs separate models for understanding and adjustment, while we adopt a unified model that jointly performs both tasks, enabling mutual enhancement.

Unified multi-modal model conducts image understanding

and generation in a unified model [8, 14, 48, 49, 51, 57, 60, 62]. Since our aim is to output both textual instructions (*i.e.*, understanding) and example images (*i.e.*, generation), we take the unified multi-modal model as our base model.

3. Task Paradigm and Dataset Construction

3.1. Task Paradigm

We first construct the task paradigm for composition guidance. Our goal is to develop an assistant that can guide humans during the photo-taking process. Therefore, we begin by revisiting how humans take photos and analyzing the key abilities the model should possess in this process.

- First, humans choose an appropriate shooting position and angle, referred to as the *vantage point*. As shown in Fig. 2c, given a scene, our model needs to infer alternative viewpoints and select the one with the best composition.
- Second, humans adjust the focal length (or zoom level on mobile photo cameras) to emphasize specific subjects. Accordingly, PhotoFramer should have the ability to identify well-composed crops within a larger scene (Fig. 2b).
- Third, humans carefully adjust the camera to maintain a level frame, avoid border distractions, and place subjects in balanced positions. Thus, as shown in Fig. 2a, PhotoFramer should position subjects appropriately (*e.g.*, centered or rule of thirds) and remove distractions to maintain clean borders.

Based on the above discussion, as illustrated in Fig. 2, we design a hierarchical task paradigm that progressively guides our PhotoFramer to acquire these capabilities:

- *Shift task*. Given a poorly composed image, PhotoFramer adjusts the framing to properly place the subject, levels the image, and removes border distractions.
- *Zoom-in task*. Given an original image, PhotoFramer generates a tighter crop with improved composition.
- *View-change task*. Given a captured scene, PhotoFramer selects a new vantage point or camera pose to reframe the scene and generates the corresponding image.

Moreover, both textual guidance and example images are important. Example images are intuitive and easy to follow, while the textual guidance provides detailed reasoning for the generated image and is easier to understand. Therefore, as depicted in Fig. 2, our PhotoFramer is designed to generate a detailed *text guidance* (describing how to improve the composition) together with an *example image* (demonstrating what a well-composed image should look like).

Formally, let the input poor-composition image be denoted as I_{poor} , the task type (*i.e.*, expressed in text) as T_{task} , the generated text guidance as T_{guide} , and the target well-composed image as I_{good} . Our PhotoFramer, denoted as $f()$, is trained to perform the following mapping: $I_{\text{good}}, T_{\text{guide}} = f(I_{\text{poor}}, T_{\text{task}})$.

3.2. Dataset Construction

Data is the key factor in training such a unified model. Following [8, 51], we need to construct $\langle T_{\text{task}}, I_{\text{poor}}$,

$I_{\text{good}}, T_{\text{guide}} \rangle$ pairs for supervision.

Task prompt collection. For T_{task} , we follow [59, 65, 66] by predefining some text templates for each task and randomly sampling one template to form the pair. For example, a template for the shift task is “shift the scene to enhance the composition”. See Appendix for all task prompts.

Image pair collection. Collecting $\langle I_{\text{poor}}, I_{\text{good}} \rangle$ image pairs is the key process and will be detailed later.

Text guidance collection. Given $\langle I_{\text{poor}}, I_{\text{good}} \rangle$ image pairs, we employ a vision-language model, Qwen2.5-VL-32B [1], to generate text guidance T_{guide} . Specifically, we input the poor and good images along with the task type, and prompt the model to describe how to transform the poor image into the good one, with detailed justifications.

Dataset statistics

Table 1. Dataset statistics.

	Shift	Zoom-in	View-change
# Original	10,321	7,665	27,393
# Pairs	164,904	14,182	

given in Tab. 1. Since the shift and zoom-in pairs are sampled from the original images in the cropping datasets (see follows), both the original images and pairs are included in the statistics. In total, our constructed dataset comprises 45K original images and 207K pairs, providing a solid foundation for model training.

3.2.1. Shift and Zoom-in Pairs

As illustrated in Fig. 3, we construct shift and zoom-in pairs from existing cropping datasets, which offers two advantages. First, the scenes and subjects in cropping datasets are curated by contributors, making them well-suited for composition-related training. Second, they contain useful annotations, which could reduce annotation workload.

Shift pair collection. We collect shift pairs from existing cropping datasets GAIC [70] and CPC [56]. GAIC provides scores for each crop, while CPC contains only selected good and best crops, which cannot be directly used. To generate missing scores in CPC, we design a mathematical sampling model in Appendix. As shown in Fig. 3, crops with scores above 4.0¹ are treated as good images, while those below 2.0 are treated as poor images, forming $\langle I_{\text{poor}}, I_{\text{good}} \rangle$ pairs. A small proportion of mid-score crops are sampled as poor images to enhance robustness. Finally, a random rotation is applied to the poor crop for augmentation. Note that our work focuses on composition instructions without changing aspect ratio. Hence, we discretize the aspect ratio range [0.45, 2.2] into 11 values, and only images with the same aspect ratio could be paired.

Zoom-in pair collection. We pair each good crop with its original image to form a $\langle I_{\text{poor}}, I_{\text{good}} \rangle^2$ pair, as depicted in Fig. 3. Thus, the key step is to identify the good crop. We adopt existing cropping datasets includ-

¹Composition scores in this work are all normalized to a [1,5] scale.

²We use “poor” for simplicity. The original image may not be strictly poor.

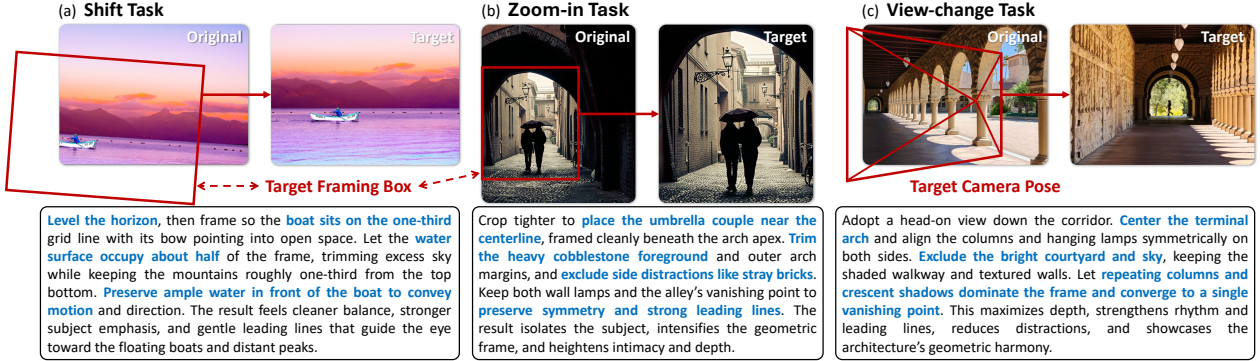


Figure 2. Task paradigm and data example. Given a poorly composed image, our PhotoFramer is required to generate a *textual guidance* (describing how to improve the composition) together with an *example image* (depicting what a well-composed image looks like). Motivated by three key photography factors (*vantage point*, *focal choice*, and *subject placement*), our PhotoFramer comprises three tasks: (a) **Shift**: adjust the framing to place the subject properly and remove border distractions; (b) **Zoom-in**: select a tighter crop (simulating a longer focal length) that yields a stronger composition; (c) **View-change**: choose a new vantage point or camera pose to reframe the scene.

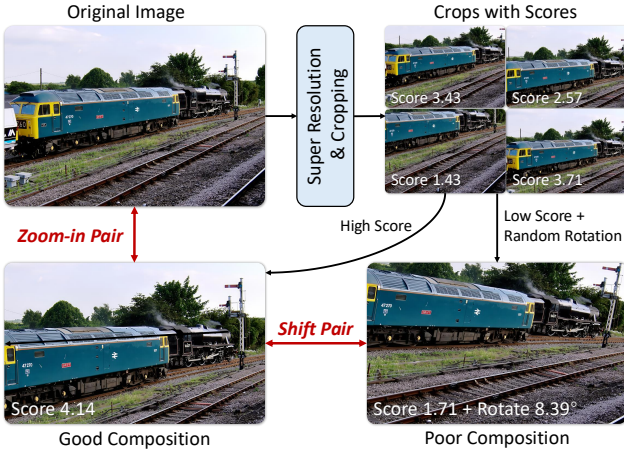


Figure 3. Dataset construction for the shift and zoom-in tasks. For the shift task, given an image from the cropping dataset, we sample its crops to form a *<poor, good>* image pair. A random rotation is applied to the poor crop. For the zoom-in task, the original image and a well-composed crop form an *<original, good>* pair. To ensure sufficient resolution, we apply $4\times$ super resolution to the original image using HYPiR [31].

ing GAIC [70], CPC [56], SACD [64], FlickrCrop [5], FLMS [10], and CUHKCrop [63]. For GAIC and CPC, where a score can be assigned to each crop, crops with scores above 4.0 are regarded as good crops. Other datasets provide a human-labeled best crop, which can be directly used. To ensure the two paired images share the same aspect ratio, we crop the original image with the largest possible region that matches the good crop’s aspect ratio. The crop center is chosen as close as possible to the image center, subject to fully containing the good crop.

Super-resolution for sufficient resolution. Some crops have very low resolution, *i.e.*, below 300 pixels, which is hard to use. Therefore, before cropping, we apply a $4\times$ super-resolution to the original image using HYPiR [31].

Image pair filtering. Three types of filtering are performed

Table 2. Results of our assessment model. Metrics for assessment and classification tasks are SRCC / PLCC and accuracy. CADB [71] and GAIC [70] datasets are for composition assessment, while AVA [38] dataset is for aesthetic assessment.

Task	Composition / Aesthetic Assessment			Classif.
	CADB	GAIC	AVA	
Dataset				CADB
Q-Align [59]	0.561 / 0.557	0.169 / 0.178	0.809 / 0.804	-
Qwen2.5-VL-32B [1]	0.420 / 0.426	0.195 / 0.205	0.527 / 0.492	0.101
Our Model (7B)	0.763 / 0.777	0.795 / 0.805	0.825 / 0.828	0.583

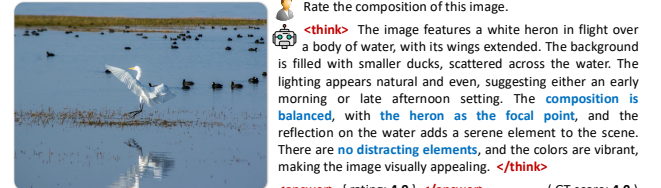


Figure 4. Qualitative results of our composition assessment model, illustrating the thinking process and final assessment output.

to ensure data quality. (1) Pairs containing any image with an aspect ratio outside $[0.45, 2.2]$ are discarded. (2) For shift pairs, we remove pairs depicting different subjects. (a) Pairs with CLIP similarity [44] below 0.8 are discarded. (b) We use U²Net [43] to extract saliency masks of the subjects, compute DINOv2 [42] features on the masked regions, and discard pairs with subject-level cosine similarity below 0.6. (c) To avoid confusion with the zoom-in task, we filter out pairs where one image is fully contained in the other and the area ratio is below 0.6. (d) To ensure sufficient composition difference in each pair, we retain those pairs whose good score exceeds the poor score by at least 0.8. (3) For zoom-in pairs, to avoid trivial cases where the good crop nearly overlaps with the original, we filter out pairs in which the good crop occupies more than 60% of the original image.

3.2.2. Composition Assessment Model

To construct the remaining view-change pairs, a good composition assessment model is necessary. As described in

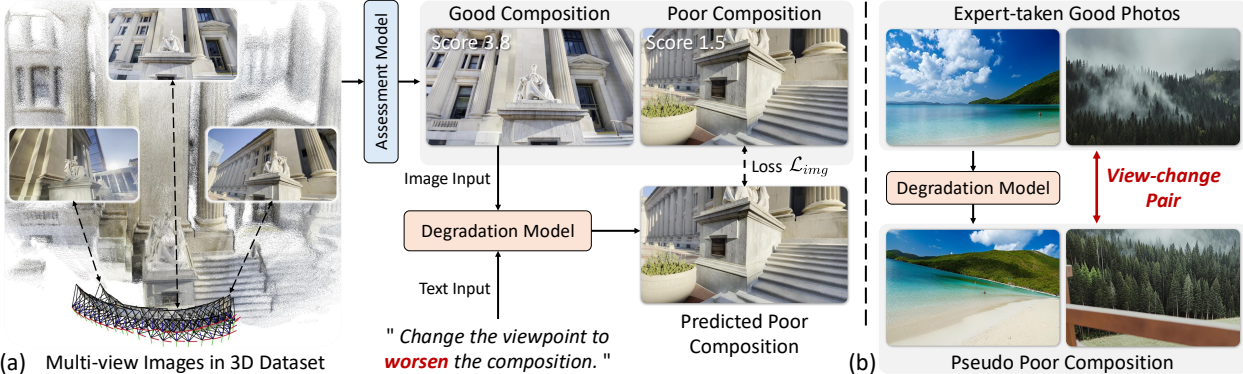


Figure 5. Dataset construction for the view-change task. (a) Leveraging our composition assessment model in Sec. 3.2.2, we sample $\langle \text{poor}, \text{good} \rangle$ image pairs from multi-view datasets. We then train a composition degradation model that generates poor-composition images from good ones. (b) We apply this degradation model to expert-taken good photos to synthesize pseudo poor-composition images, forming the final pairs. We do not rely solely on multi-view datasets, as most of their good images are not sufficiently well-composed.

Sec. 3.2.1, the shift and zoom-in pairs are built upon cropping datasets with human-provided annotations. However, most in-the-wild images lack such annotations.

Composition assessment dataset. To train such an assessment model, we primarily use composition scoring datasets, CADB [71] and GAIC [70], and additionally incorporate composition classification datasets, CADB [71] and KU-PCP [25], and the aesthetic assessment dataset AVA [38], given their strong relevance to composition assessment.

Composition assessment model. Following [30, 61], we adopt Qwen2.5-VL-7B [1] as the base and train it using the GRPO [46] reinforcement learning algorithm. The assessment and classification results are presented in Tab. 2. Our 7B model outperforms both Q-Align [59] (aesthetic mode) and the much larger Qwen2.5-VL-32B [1]. One qualitative example is shown in Fig. 4, where our model provides detailed reasoning alongside the composition score.

3.2.3. View-change Pairs

Pair collection from multi-view data. A natural source to sample image pairs with varying viewpoints is 3D datasets containing multi-view images. DL3DV-10K [32] is a large-scale 3D dataset comprising 10K scenes and 51M frames. As shown in Fig. 5, we evaluate images within each scene using our assessment model, then select up to three best images and ten worst images to form pairs. However, even the best frames often lack expert-level composition quality, making it insufficient to rely solely on this dataset.

Pair collection from expert-taken photos. Multi-view data can provide image pairs, but the good images often lack strong composition quality. In contrast, expert-taken photos exhibit good composition but lack corresponding poor images to form pairs. Thus, as shown in Fig. 5, we use the expert-taken photo as good image, and generate a poor view of this image, forming the view-change pair.

– *Composition degradation model.* In the first stage, we use the pairs from 3D dataset to train a degradation model (the

same to the final model introduced in Sec. 4). As depicted in Fig. 5a, the model takes a well-composed image along with a degradation instruction such as “Change the viewpoint to *worsen* the composition”, and generates the corresponding poor-composition image. An image reconstruction loss between the predicted poor image and the ground-truth poor image is minimized to optimize the model.

– *Degradation on excellent images.* As shown in Fig. 5b, in the second stage, we apply the trained degradation model to human-taken photos to synthesize pseudo poor images, forming the final pairs. We use two sources of good images: the Unsplash Lite dataset [9] with 25K professional photographs, and another 10K images taken by ourselves. The Unsplash Lite dataset reflects professional-level photography, while our own dataset represents the level of amateur photography, providing complementary data diversity.

Image pair filtering. We perform three types of filtering to ensure data quality. (1) The first discards pairs containing any image with an extreme aspect ratio outside [0.45, 2.2]. (2) The second aims to ensure the quality of good images. (a) File size: we discard images smaller than 200 KB (JPG, 1024 resolution, quality 95), as such images are often overly simplistic (*e.g.*, plain colors or curves). (b) Image quality: images with a DeQA-Score [67] below 3.5 are removed. (c) Composition: only images with a composition score above 3.0 are retained. (d) Art: for the Unsplash Lite dataset [9], we filter out images with keywords like “abstract”, “painting”, and “art”, as our focus is on real-world scenes. (3) The third aims to enforce view consistency within each image pair. VGGT [54] is employed to compute the Field-of-View (FoV) overlap between pairs. Low FoV intersection means poor spatial correspondence and thus leads to exclusion.

4. PhotoFramer Model

Model architecture. As stated in Sec. 3.1, our goal is to predict both a textual instruction and a well-composed example image. Bagel [8] is a unified multi-modal model

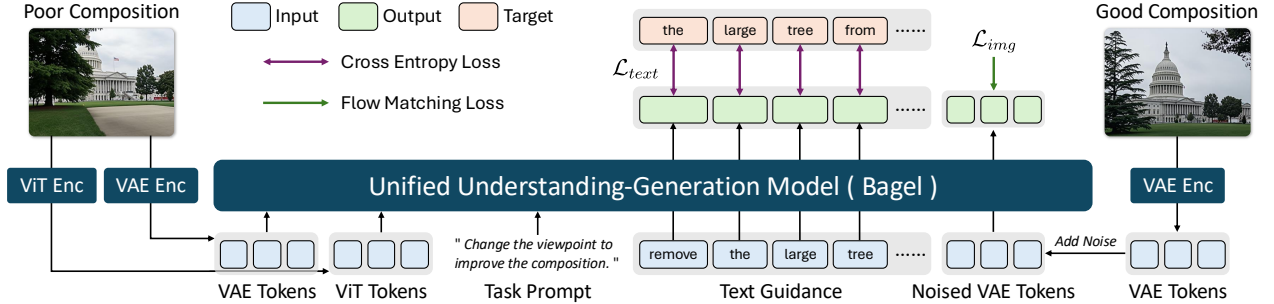


Figure 6. PhotoFramer architecture. We adopt Bagel [8], a unified understanding-generation model, as the base model. Given a task prompt and a poorly composed image, the model predicts both text guidance and a well-composed example image. The text guidance is optimized using a cross-entropy loss \mathcal{L}_{text} for next-token prediction, while the example image is trained using a flow matching loss \mathcal{L}_{img} .

capable of producing both textual and visual outputs, with strong language understanding, visual perception, and image generation capabilities. Therefore, we adopt Bagel as our base model for finetuning. As illustrated in Fig. 6, given a task prompt and a poorly composed image, the model predicts a textual instruction and a well-composed example image. For visual input, Bagel uses two types of vision tokens: VAE tokens encoded by the FLUX VAE [23] and ViT tokens extracted by the SigLIP2-so400m/14 [52] ViT model. The VAE tokens, containing pixel-level information, are used for image generation, while the ViT tokens, encoding semantic information, are leveraged for visual understanding. The textual instruction is optimized with a cross-entropy loss \mathcal{L}_{text} for next-token prediction, and the example image is optimized with a flow-matching loss \mathcal{L}_{img} . Note that the generated image attends to the textual instruction through the attention mechanism, enabling instruction-driven example image generation. For further architectural details of Bagel, we refer the reader to [8].

Auto prompt design. As shown in Fig. 2, PhotoFramer supports three sub-tasks. Each task uses predefined prompt templates. However, this requires users to explicitly specify the task type, which can be inconvenient. To alleviate this issue, we adopt *auto prompts* such that the user does not need to indicate the task. We propose two types of auto prompts: (1) *Static auto task*, where users may not want to change their viewpoint, thus only shift and zoom-in are allowed. (2) *Full auto task*, where all three tasks could be applied. For static auto prompts, we use, *e.g.*, “Refine the composition through shift or zoom-in adjustments”. For full auto prompts, we use free-form instructions such as “Capture this scene with better composition”. More examples are provided in Appendix. During training, task-specific prompts are randomly replaced by auto prompts, enabling the model to self-determine the most suitable operations.

Inference. The inference process consists of two stages. (1) *Understanding*. The model takes visual tokens and a task prompt as inputs, analyzes the current composition, and predicts text guidance describing how to improve it. (2) *Generation*. The predicted text guidance is first appended

to the inputs. Starting from pure noise tokens, the model progressively denoises to generate latent tokens. After VAE decoding, a well-composed example image is obtained.

5. Experiments

5.1. Metrics and Details

Evaluation of example images. Assessing composition is non-trivial. Although we have trained a composition assessment model, it was used in our dataset construction and thus would bias the evaluation. As noted in [21, 66], humans find it easier to compare two images than to rate a single one. Therefore, we evaluate each generated example by comparing it with both the original and ground-truth images. The comparison is conducted by GPT-5 [41] and humans, and the two win rates are reported as the metric. We manually select and carefully examine 200 to 300 samples for each task to construct a benchmark to compute the metric.

Evaluation of text guidance. We evaluate the consistency between the text guidance and the corresponding example images. Specifically, we input the original image, the model-improved example image, and the model-predicted text guidance into GPT-5 [41], and request an evaluation score indicating how accurately the text guidance describes the change from the original image to the example image.

Implementation details. We follow the training setup of Bagel [8] to train our model. The VAE encoder and decoder are kept frozen, while the ViT encoder and the main model remain trainable. Training is performed on 8 NVIDIA A100 GPUs using the AdamW optimizer [19] with a batch size of 8, a learning rate of 2e-5, and 50K training steps. An exponential moving average with a decay rate of 0.9999 is applied to stabilize training. The two loss terms, \mathcal{L}_{text} and \mathcal{L}_{img} , are assigned equal weights. All images are resized to a 512 shorter side while preserving the aspect ratio. During inference, the number of image generation steps is set to 30.

5.2. Comparison Results

Baselines. We compare with state-of-the-art editing models, including Kontext [2] and Qwen-Image-Edit [58]. The original unified model Bagel [8] is also included, along with

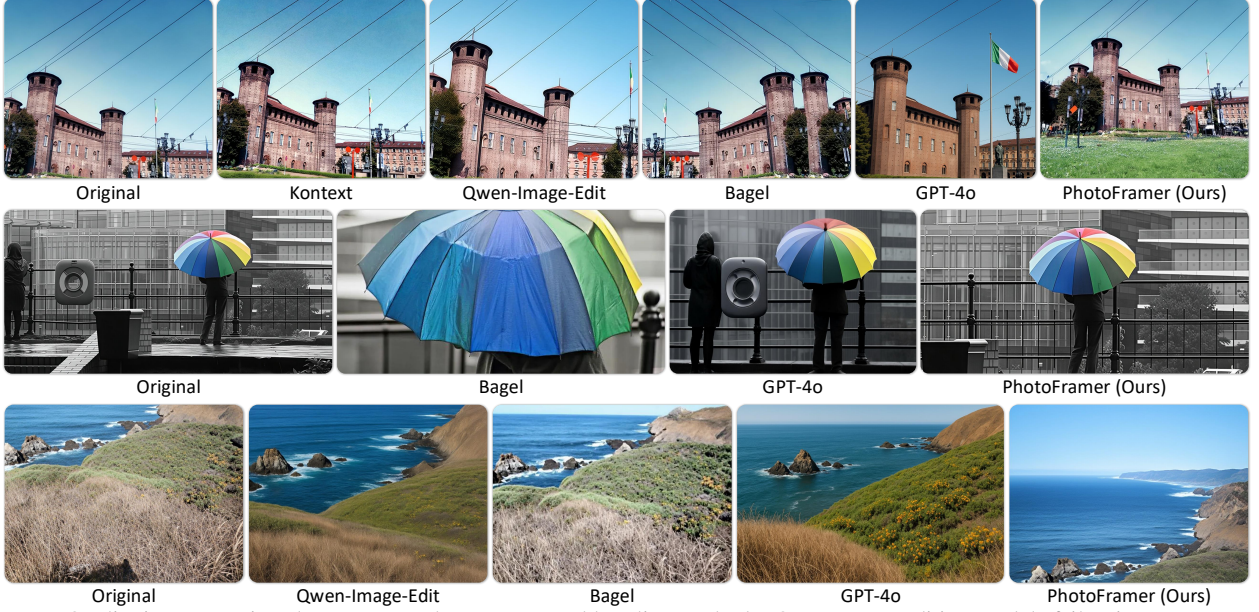


Figure 7. Qualitative comparison between our PhotoFramer and baseline methods. Open-source editing models fail to improve composition. GPT-4o [40] could generate well-composed images but with low fidelity (*i.e.*, it alters semantic details of the original image).

Table 3. Quantitative results of model-generated example images on our benchmark. We compare the model-generated example images with their original images / ground-truth images, evaluated by both GPT-5 [41] and humans. The win rate (%) is reported as the metric. We also report image quality assessment (with DeQA-Score [67]) and image aesthetic assessment (with Q-Align [59]) results for reference.

Method	Shift Task		Zoom-in Task ¹		View-change Task		Quality DeQA [59]	Aesthetic Q-Align [59]
	GPT-5 [41]	Human	GPT-5 [41]	Human	GPT-5 [41]	Human		
Kontext [2]	39.88 / 12.27	49.69 / 4.94	- / 15.52	- / 5.17	46.74 / 15.76	48.37 / 5.98	3.88	3.13
Qwen-Image-Edit [58]	46.01 / 16.56	48.43 / 10.49	- / 39.65	- / 13.79	70.65 / 36.96	61.96 / 20.65	4.03	3.29
Bagel [8]	27.61 / 14.73	38.36 / 8.02	- / 22.41	- / 12.07	47.28 / 14.13	64.13 / 15.22	3.87	3.08
GPT-4o [40]	69.93 / 33.99	68.46 / 22.37	- / 52.73	- / 27.27	84.61 / 51.65	81.52 / 41.30	3.97	3.26
PhotoFramer (Ours)	80.37 / 35.58	88.05 / 43.83	- / 67.24	- / 48.28	82.07 / 50.54	85.87 / 47.28	4.07	3.17

¹ For the zoom-in task, we **exclude** Zoomed *vs.* Original because the pair is trivially detectable (*i.e.*, through scale/cropping cues), which induces type preference and inflates win rates. We therefore report only Zoomed *vs.* Ground-Truth win rate.

the powerfully proprietary GPT-4o³ [40]. We adopt Bagel’s reasoning-based editing mode, which first generates textual edit instructions and then edits the image accordingly.

Quantitative results of example images are presented in Tab. 3. First, open-source editing models fail to improve composition, exhibiting low win rates against both the original and ground-truth images. Second, in the view-change task, where the models have greater freedom in generation, their performance is substantially improved. Third, GPT-4o achieves substantially better results than open-source models, demonstrating strong generalization ability to this new task. However, GPT-4o often alters semantic details of the original image, as depicted in Fig. 7. Finally, our PhotoFramer outperforms open-source methods with the highest win rates, and matches or even surpasses GPT-4o. Tab. 3 demonstrates that our model not only improves composition but also preserves high-level image quality and aesthetics. The qualitative examples in Fig. 1 and Fig. 7 fur-

Table 4. Quantitative results of consistency between the model-predicted text guidance and corresponding example images.

Task	Shift	Zoom-in	View-change	Average
Bagel [8]	77.01	84.82	87.47	83.10
PhotoFramer (Ours)	91.96	92.59	91.52	92.02

ther show that PhotoFramer effectively enhances composition while maintaining high fidelity to the original content.

Evaluation results of text guidance are provided in Tab. 4. The original Bagel model has exhibited reasonable consistency between text guidance and the corresponding example images across the three composition instruction sub-tasks. After finetuning on our constructed datasets, this consistency is further and stably improved (92.02% *vs.* 83.10%).

5.3. Ablation Studies and Discussions

Text guidance alone is not enough. A natural question arises for the unified framework: can we rely solely on the text guidance and feed it into other editing models to generate example images? As shown in Fig. 8, our generated text guidance cannot be directly utilized by Qwen-Image-

³We use the API version “gpt-image-1”.

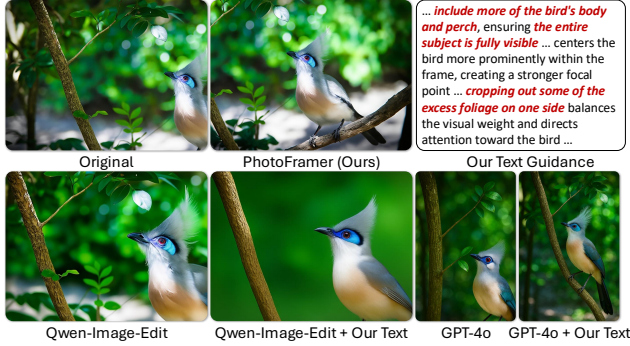


Figure 8. Our generated text guidance cannot be directly utilized by Qwen-Image-Edit, even though it employs an LLM as the text encoder. In contrast, GPT-4o benefits from our text guidance (*i.e.*, including the entire body of the bird), albeit with lower fidelity.



Figure 9. Illustration of auto prompt. Given an auto prompt “refine the composition using shift or zoom-in”, our model does not merely select one task type but adaptively fuses multiple operations to produce a better composition. Text guidance is omitted.

Edit, though it employs a Large Language Model (LLM) as the text encoder. Moreover, directly using our text guidance even degrades the fidelity of example images. In contrast, when provided with our text guidance (*i.e.*, “include more of the bird’s body and perch”), GPT-4o successfully includes the entire bird, demonstrating strong instruction-following ability. However, its fidelity remains unsatisfactory.

Example image alone is not enough. First, as depicted in Fig. 10, textual guidance plays a crucial role in generating example images. Even revising a few key words could lead to dramatically different results. Second, we train Bagel using only image pairs without text guidance. As illustrated in Fig. 11, without textual input, the model fails to remove the foreground fence, although it successfully includes the sky. In contrast, when trained with text guidance, the model explicitly learns to “remove the fence” and successfully follows this instruction to generate a better example image. Third, we fine-tune Kontext (which does not support tex-



Figure 10. Text guidance is important for image generation. If we manually revise a few key words (*i.e.*, remove “upper”, add “including lower body”), the generated image will be quite different.



Figure 11. Training without text guidance fails to remove the fence distractions, although it successfully includes the sky, whereas training with text guidance predicts to “remove the fence” in textual output and generates a well-composed image without fence.



Figure 12. Finetuned Bagel (*i.e.*, on both textual and visual data) successfully includes the *whole* wooden house as in the text guidance, outperforming finetuned Kontext (*i.e.*, on visual data only).



Figure 13. A failure case where our PhotoFramer misinterprets a painting as a real photograph and attempts to refine the composition by removing the “background” (*i.e.*, the painting frame).

tual training) using our collected image pairs. As shown in Fig. 12, Kontext can partially shift the wooden house toward the center but fails to include it entirely. In contrast, the finetuned Bagel predicts to “include the *whole* wooden structure” and generates a well-composed image accordingly.

Task prompt. As illustrated at the top of Fig. 9, different task prompts lead PhotoFramer to apply different operations to improve composition. Notably, as shown at the bottom of Fig. 9, when specific tasks fail, the auto task can still produce strong results. The original image was randomly taken in a city and contains a distraction (*i.e.*, the back of a half-visible woman). The shift task mistakenly treats this distraction as the main subject and attempts to center it, while the zoom-in task crops too tightly, cutting off the top of the building. With the auto prompt, where the model can adap-

tively apply shift and/or zoom-in, PhotoFramer effectively fuses multiple adjustments to achieve a better composition.

Failure cases. We present a failure case in Fig. 13 where PhotoFramer misinterprets a painting as a real photograph and attempts to refine the composition by removing the perceived “background” (*i.e.*, the painting frame). This occurs because most painting images were excluded from training.

6. Conclusions

We introduce PhotoFramer, a multi-modal composition instruction model built upon a hierarchical task paradigm, curated datasets, and a unified understanding-generation framework, to guide photographic composition through actionable textual instructions and example image generation.

References

- [1] Shuai Bai, Keqin Chen, Xuejing Liu, Jialin Wang, Wenbin Ge, Sibo Song, Kai Dang, Peng Wang, Shijie Wang, Jun Tang, et al. Qwen2.5-VL technical report. *arXiv preprint arXiv:2502.13923*, 2025. [2](#), [3](#), [4](#), [5](#), [13](#), [14](#)
- [2] Stephen Batifol, Andreas Blattmann, Frederic Boesel, Saksham Consul, Cyril Diagne, Tim Dockhorn, Jack English, Zion English, Patrick Esser, Sumith Kulal, et al. FLUX.1 Kontext: Flow matching for in-context image generation and editing in latent space. *arXiv preprint arXiv:2506.15742*, 2025. [2](#), [6](#), [7](#)
- [3] Mingdeng Cao, Xuaner Zhang, Yinqiang Zheng, and Zhihao Xia. Instruction-based image manipulation by watching how things move. In *CVPR*, 2025. [2](#)
- [4] Shuo Cao, Nan Ma, Jiayang Li, Xiaohui Li, Lihao Shao, Kaiwen Zhu, Yu Zhou, Yuandong Pu, Jiarui Wu, Jiaquan Wang, et al. ArtiMuse: Fine-grained image aesthetics assessment with joint scoring and expert-level understanding. *arXiv preprint arXiv:2507.14533*, 2025. [2](#)
- [5] Yi-Ling Chen, Tzu-Wei Huang, Kai-Han Chang, Yu-Chen Tsai, Hwann-Tzong Chen, and Bing-Yu Chen. Quantitative analysis of automatic image cropping algorithms: A dataset and comparative study. In *WACV*, 2017. [2](#), [4](#)
- [6] Yi-Ling Chen, Jan Klopp, Min Sun, Shao-Yi Chien, and Kwan-Liu Ma. Learning to compose with professional photographs on the web. In *ACM MM*, 2017. [2](#)
- [7] Mauricio Delbracio, Damien Kelly, Michael S Brown, and Peyman Milanfar. Mobile computational photography: A tour. *Annual Review of Vision Science*, 2021. [1](#)
- [8] Chaorui Deng, Deyao Zhu, Kunchang Li, Chenhui Gou, Feng Li, Zeyu Wang, Shu Zhong, Weihao Yu, Xiaonan Nie, Ziang Song, et al. Emerging properties in unified multimodal pretraining. *arXiv preprint arXiv:2505.14683*, 2025. [2](#), [3](#), [5](#), [6](#), [7](#)
- [9] Unsplash Developers. Unsplash lite dataset 1.3.0, 2020. [2](#), [5](#), [16](#)
- [10] Chen Fang, Zhe Lin, Radomir Mech, and Xiaohui Shen. Automatic image cropping using visual composition, boundary simplicity and content preservation models. In *ACM MM*, 2014. [2](#), [4](#), [14](#)
- [11] Farshid Farhat, Mohammad Mahdi Kamani, Sahil Mishra, and James Z Wang. Intelligent portrait composition assistance: Integrating deep-learned models and photography idea retrieval. In *ACM MM Workshops*, 2017. [2](#)
- [12] Farshid Farhat, Mohammad Mahdi Kamani, and James Z Wang. CAPTAIN: Comprehensive composition assistance for photo taking. *ACM Transactions on Multimedia Computing, Communications, and Applications*, 2022. [2](#)
- [13] Michael Freeman. *The Photographer’s Eye Digitally Remastered 10th Anniversary Edition: Composition and Design for Better Digital Photos*. Routledge, 2017. [2](#)
- [14] Yuying Ge, Sijie Zhao, Jinguo Zhu, Yixiao Ge, Kun Yi, Lin Song, Chen Li, Xiaohan Ding, and Ying Shan. SEED-X: Multimodal models with unified multi-granularity comprehension and generation. *arXiv preprint arXiv:2404.14396*, 2024. [2](#), [3](#)
- [15] Guanjun Guo, Hanzi Wang, Chunhua Shen, Yan Yan, and Hong-Yuan Mark Liao. Automatic image cropping for visual aesthetic enhancement using deep neural networks and cascaded regression. *IEEE TMM*, 2018. [2](#)
- [16] Chaoyi Hong, Shuaiyuan Du, Ke Xian, Hao Lu, Zhiguo Cao, and Weicai Zhong. Composing photos like a photographer. In *CVPR*, 2021. [2](#)
- [17] James Hong, Lu Yuan, Michaël Gharbi, Matthew Fisher, and Kayvon Fatahalian. Learning subject-aware cropping by out-painting professional photos. In *AAAI*, 2024. [2](#)
- [18] Andrey Ignatov, Georgii Perevozchikov, Radu Timofte, Cheng Li, Lian Liu, Jun Cao, Heng Sun, Wu Pan, Song Wang, KeQiang Yu, et al. Learned smartphone ISP on mobile GPUs, mobile AI 2025 challenge: Report. In *CVPR Workshops*, 2025. [1](#)
- [19] Loschilov Ilya and Hutter Frank. Decoupled weight decay regularization. In *ICLR*, 2019. [6](#), [14](#)
- [20] Gengyun Jia, Huaibo Huang, Chaoyou Fu, and Ran He. Rethinking image cropping: Exploring diverse compositions from global views. In *CVPR*, 2022. [2](#)
- [21] Gu Jinjin, Cai Haoming, Chen Haoyu, Ye Xiaoxing, Jimmy S Ren, and Dong Chao. PIPAL: A large-scale image quality assessment dataset for perceptual image restoration. In *ECCV*, 2020. [6](#)
- [22] Diederik P Kingma. Adam: A method for stochastic optimization. In *ICLR*, 2015. [12](#)
- [23] Black Forest Labs. GPT-4V(ision) system card, 2024. [6](#)
- [24] Michael Langford. *Basic photography*. Routledge, 2013. [2](#)
- [25] Jun-Tae Lee, Han-Ul Kim, Chul Lee, and Chang-Su Kim. Photographic composition classification and dominant geometric element detection for outdoor scenes. *Journal of Visual Communication and Image Representation*, 2018. [2](#), [5](#), [12](#)
- [26] Debang Li, Huikai Wu, Junge Zhang, and Kaiqi Huang. A2-RL: Aesthetics aware reinforcement learning for image cropping. In *CVPR*, 2018. [2](#)
- [27] Debang Li, Junge Zhang, and Kaiqi Huang. Learning to learn cropping models for different aspect ratio requirements. In *CVPR*, 2020. [2](#)
- [28] Debang Li, Junge Zhang, Kaiqi Huang, and Ming-Hsuan Yang. Composing good shots by exploiting mutual relations. In *CVPR*, 2020. [2](#)

- [29] Jiawan Li, Fei Zhou, Zhipeng Zhong, Jiongshi Lin, and Guoping Qiu. Towards smart point-and-shoot photography. In *CVPR*, 2025. 2
- [30] Weiqi Li, Xuanyu Zhang, Shijie Zhao, Yabin Zhang, Junlin Li, Li Zhang, and Jian Zhang. Q-Insight: Understanding image quality via visual reinforcement learning. In *NeurIPS*, 2025. 5, 13
- [31] Xinqi Lin, Fanghua Yu, Jinfan Hu, Zhiyuan You, Wu Shi, Jimmy S Ren, Jinjin Gu, and Chao Dong. Harnessing diffusion-yielded score priors for image restoration. *ACM TOG*, 2025. 4, 14
- [32] Lu Ling, Yichen Sheng, Zhi Tu, Wentian Zhao, Cheng Xin, Kun Wan, Lantao Yu, Qianyu Guo, Zixun Yu, Yawen Lu, et al. DL3DV-10k: A large-scale scene dataset for deep learning-based 3d vision. In *CVPR*, 2024. 2, 5, 14
- [33] Boyang Liu, Yifan Hu, Senjie Jin, Shihan Dou, Ginglei Shi, Jie Shao, Tao Gui, and Xuanjing Huang. Unlocking the essence of beauty: Advanced aesthetic reasoning with relative-absolute policy optimization. *arXiv preprint arXiv:2509.21871*, 2025. 2
- [34] Dong C Liu and Jorge Nocedal. On the limited memory bfgs method for large scale optimization. *Mathematical Programming*, 1989. 12
- [35] Haotian Liu, Chunyuan Li, Qingyang Wu, and Yong Jae Lee. Visual instruction tuning. In *NeurIPS*, 2024. 2
- [36] Xiaoyu Liu, Ming Liu, Junyi Li, Shuai Liu, Xiaotao Wang, Lei Lei, and Wangmeng Zuo. Beyond image borders: Learning feature extrapolation for unbounded image composition. In *ICCV*, 2023. 2
- [37] Chamin Morikawa, Michihiro Kobayashi, Masaki Satoh, Yasuhiro Kuroda, Teppei Inomata, Hitoshi Matsuo, Takeshi Miura, and Masaki Hilaga. Image and video processing on mobile devices: a survey. *The Visual Computer*, 2021. 1
- [38] Naila Murray, Luca Marchesotti, and Florent Perronnin. AVA: A large-scale database for aesthetic visual analysis. In *CVPR*, 2012. 4, 5, 12
- [39] OpenAI. GPT-4V(ision) system card, 2023. 2
- [40] OpenAI. GPT-4o system card. *arXiv preprint arXiv:2410.21276*, 2024. 7
- [41] OpenAI. GPT-5 system card, 2025. 6, 7
- [42] Maxime Oquab, Timothée Darcet, Théo Moutakanni, Huy Vo, Marc Szafraniec, Vasil Khalidov, Pierre Fernandez, Daniel Haziza, Francisco Massa, Alaeldin El-Nouby, et al. DINOV2: Learning robust visual features without supervision. *Transactions on Machine Learning Research*, 2024. 4
- [43] Xuebin Qin, Zichen Zhang, Chenyang Huang, Masood Dehghan, Osmar R Zaiane, and Martin Jagersand. U²-Net: Going deeper with nested u-structure for salient object detection. *PR*, 2020. 4
- [44] Alec Radford, Jong Wook Kim, Chris Hallacy, Aditya Ramesh, Gabriel Goh, Sandhini Agarwal, Girish Sastry, Amanda Askell, Pamela Mishkin, Jack Clark, et al. Learning transferable visual models from natural language supervision. In *ICML*, 2021. 4
- [45] Robin Rombach, Andreas Blattmann, Dominik Lorenz, Patrick Esser, and Björn Ommer. High-resolution image synthesis with latent diffusion models. In *CVPR*, 2022. 2
- [46] Zhihong Shao, Peiyi Wang, Qihao Zhu, Runxin Xu, Junxiao Song, Xiao Bi, Haowei Zhang, Mingchuan Zhang, YK Li, Yang Wu, et al. DeepseekMath: Pushing the limits of mathematical reasoning in open language models. *arXiv preprint arXiv:2402.03300*, 2024. 5, 13
- [47] Yukun Su, Yiwen Cao, Jingliang Deng, Fengyun Rao, and Qingyao Wu. Spatial-semantic collaborative cropping for user generated content. In *AAAI*, 2024. 2
- [48] Quan Sun, Qiyi Yu, Yufeng Cui, Fan Zhang, Xiaosong Zhang, Yueze Wang, Hongcheng Gao, Jingjing Liu, Tiejun Huang, and Xinlong Wang. Emu: Generative pretraining in multimodality. In *ICLR*, 2024. 3
- [49] Chameleon Team. Chameleon: Mixed-modal early-fusion foundation models. *arXiv preprint arXiv:2405.09818*, 2024. 2, 3
- [50] DXOMARK Team. DXOMARK - quality testing, scores and reviews, 2025. 1
- [51] Shengbang Tong, David Fan, Jiachen Zhu, Yunyang Xiong, Xinlei Chen, Koustuv Sinha, Michael Rabbat, Yann LeCun, Saining Xie, and Zhuang Liu. MetaMorph: Multimodal understanding and generation via instruction tuning. *arXiv preprint arXiv:2412.14164*, 2024. 3
- [52] Michael Tschanne, Alexey Gritsenko, Xiao Wang, Muhammad Ferjad Naeem, Ibrahim Alabdulmohsin, Nikhil Parthasarathy, Talfan Evans, Lucas Beyer, Ye Xia, Basil Mustafa, et al. SigLIP 2: Multilingual vision-language encoders with improved semantic understanding, localization, and dense features. *arXiv preprint arXiv:2502.14786*, 2025. 6
- [53] Yi Tu, Li Niu, Weijie Zhao, Dawei Cheng, and Liqing Zhang. Image cropping with composition and saliency aware aesthetic score map. In *AAAI*, 2020. 2
- [54] Jianyuan Wang, Minghao Chen, Nikita Karaev, Andrea Vedaldi, Christian Rupprecht, and David Novotny. VGGT: Visual geometry grounded transformer. In *CVPR*, 2025. 5
- [55] Wenguan Wang and Jianbing Shen. Deep cropping via attention box prediction and aesthetics assessment. In *ICCV*, 2017. 2
- [56] Zijun Wei, Jianming Zhang, Xiaohui Shen, Zhe Lin, Radomir Mech, Minh Hoai, and Dimitris Samaras. Good view hunting: Learning photo composition from dense view pairs. In *CVPR*, 2018. 2, 3, 4, 11, 14
- [57] Chengyue Wu, Xiaokang Chen, Zhiyu Wu, Yiyang Ma, Xingchao Liu, Zizheng Pan, Wen Liu, Zhenda Xie, Xingkai Yu, Chong Ruan, et al. Janus: Decoupling visual encoding for unified multimodal understanding and generation. In *CVPR*, 2025. 3
- [58] Chenfei Wu, Jiahao Li, Jingren Zhou, Junyang Lin, Kaiyuan Gao, Kun Yan, Sheng-ming Yin, Shuai Bai, Xiao Xu, Yilei Chen, et al. Qwen-Image technical report. *arXiv preprint arXiv:2508.02324*, 2025. 6, 7
- [59] Haoning Wu, Zicheng Zhang, Weixia Zhang, Chaofeng Chen, Liang Liao, Chunyi Li, Yixuan Gao, Annan Wang, Erli Zhang, Wenxiu Sun, et al. Q-Align: Teaching LMMs for visual scoring via discrete text-defined levels. In *ICML*, 2024. 3, 4, 5, 7

- [60] Shengqiong Wu, Hao Fei, Leigang Qu, Wei Ji, and Tat-Seng Chua. NExT-GPT: Any-to-any multimodal llm. In *ICML*, 2024. 2, 3
- [61] Tianhe Wu, Jian Zou, Jie Liang, Lei Zhang, and Kede Ma. Visualquality-r1: Reasoning-induced image quality assessment via reinforcement learning to rank. In *NeurIPS*, 2025. 5, 13
- [62] Jinheng Xie, Weijia Mao, Zechen Bai, David Junhao Zhang, Weihao Wang, Kevin Qinghong Lin, Yuchao Gu, Zhijie Chen, Zhenheng Yang, and Mike Zheng Shou. Show-o: One single transformer to unify multimodal understanding and generation. In *ICLR*, 2025. 2, 3
- [63] Jianzhou Yan, Stephen Lin, Sing Bing Kang, and Xiaou Tang. Learning the change for automatic image cropping. In *CVPR*, 2013. 2, 4, 14
- [64] Guo-Ye Yang, Wen-Yang Zhou, Yun Cai, Song-Hai Zhang, and Fang-Lue Zhang. Focusing on your subject: Deep subject-aware image composition recommendation networks. *Computational Visual Media*, 2023. 2, 4, 14
- [65] Zhiyuan You, Jinjin Gu, Zheyuan Li, Xin Cai, Kaiwen Zhu, Chao Dong, and Tianfan Xue. Descriptive image quality assessment in the wild. *arXiv preprint arXiv:2405.18842*, 2024. 3
- [66] Zhiyuan You, Zheyuan Li, Jinjin Gu, Zhenfei Yin, Tianfan Xue, and Chao Dong. Depicting beyond scores: Advancing image quality assessment through multi-modal language models. In *ECCV*, 2024. 3, 6
- [67] Zhiyuan You, Xin Cai, Jinjin Gu, Tianfan Xue, and Chao Dong. Teaching large language models to regress accurate image quality scores using score distribution. In *CVPR*, 2025. 5, 7
- [68] Peter Young, Alice Lai, Micah Hodosh, and Julia Hockenmaier. From image descriptions to visual denotations: New similarity metrics for semantic inference over event descriptions. *Transactions of the Association for Computational Linguistics*, 2014. 14
- [69] Hui Zeng, Lida Li, Zisheng Cao, and Lei Zhang. Reliable and efficient image cropping: A grid anchor based approach. In *CVPR*, 2019. 2
- [70] Hui Zeng, Lida Li, Zisheng Cao, and Lei Zhang. Grid anchor based image cropping: A new benchmark and an efficient model. *IEEE TPAMI*, 2020. 2, 3, 4, 5, 12, 14
- [71] Bo Zhang, Li Niu, and Liqing Zhang. Image composition assessment with saliency-augmented multi-pattern pooling. In *BMVC*, 2021. 2, 4, 5, 12
- [72] Bo Zhang, Li Niu, Xing Zhao, and Liqing Zhang. Human-centric image cropping with partition-aware and content-preserving features. In *ECCV*, 2022. 2
- [73] Ke Zhang, Tianyu Ding, Jiachen Jiang, Tianyi Chen, Ilya Zharkov, Vishal M Patel, and Luming Liang. ProCrop: Learning aesthetic image cropping from professional compositions. *arXiv preprint arXiv:2505.22490*, 2025. 2
- [74] Xiaoyan Zhang, Zhuopeng Li, Martin Constable, Kap Luk Chan, Zhenhua Tang, and Gaoyang Tang. Pose-based composition improvement for portrait photographs. *IEEE TCSVT*, 2018. 2
- [75] Zhaoran Zhao, Peng Lu, Anran Zhang, Peipei Li, Xia Li, Xuannan Liu, Yang Hu, Shiyi Chen, Liwei Wang, and Wenhao Guo. Can machines understand composition? dataset and benchmark for photographic image composition embedding and understanding. In *CVPR*, 2025. 2
- [76] Deyao Zhu, Jun Chen, Xiaoqian Shen, Xiang Li, and Mohamed Elhoseiny. MiniGPT-4: Enhancing vision-language understanding with advanced large language models. In *ICLR*, 2024. 2
- [77] Jinguo Zhu, Weiyun Wang, Zhe Chen, Zhaoyang Liu, Shenglong Ye, Lixin Gu, Hao Tian, Yuchen Duan, Weijie Su, Jie Shao, et al. InternVL3: Exploring advanced training and test-time recipes for open-source multimodal models. *arXiv preprint arXiv:2504.10479*, 2025. 2

Appendix

A. More Results

We have added more qualitative results in Figs. A9 to A11, including the poorly composed input, the predicted text guidance, and the model-generated well-composed image, for all three sub-tasks. In the predicted text guidance, actionable suggestions are highlighted in **blue**, while hallucinated descriptions are marked in **red**. Overall, our PhotoFramer could provide clear and practically useful composition suggestions that correspond well to the generated example well-composed images. However, in some cases, small hallucinations still occur. For instance, in the shift task, the model may confuse left and right directions, leading to incorrect spatial descriptions.

B. More Details of Dataset Construction

In this section, we provide more details of our dataset construction, including the optimization to obtain composition scores for CPC dataset (Sec. B.1), composition assessment model training (Sec. B.2), details of view-change pairs collection (Sec. B.3), more dataset statistics (Sec. B.4), and task prompt details (Sec. B.5).

B.1. Score Optimization of CPC Dataset

As stated in Sec. 3.2.1 of the main paper, the composition scores are required for each crop to construct shift or zoom-in pairs. However, the CPC dataset [56] contains only selected good and best crops, which cannot be directly used to construct the pairs. Therefore, we build a mathematical model to infer scores for all crops.

Annotation of CPC dataset. Given an original image and its N crops ($N=24$ in CPC), one annotator first selects 8~20 good crops, and then chooses the 3 best crops from these good ones. Each image is annotated by 6 annotators. By averaging the annotations from the 6 annotators, we obtain the probability that crop i is good, p_i^{good} , and the probability that it belongs to the top-3 set, p_i^{top3} .

Assumption. Annotators are required to select 8~20 good crops out of all 24 crops, where good crops constitute a relatively large proportion. Therefore, we assume that a crop i is considered good if its score s_i exceeds a threshold, and this decision *depends only on its own quality without pairwise comparison*. In contrast, selecting the top-3 crops requires careful comparison among candidates. Thus, the decision necessarily *depends on relative scores between crops*.

Mathematical modeling. According to the above assumption, whether a crop is considered good or not *depends only on its own quality without pairwise comparison*. Therefore, we directly model the probability of a crop being good as a sigmoid function of its own score:

$$\hat{p}_i^{\text{good}} = \sigma(s_i), \quad (\text{A1})$$

where $\sigma(\cdot)$ denotes the sigmoid activation function.

For the top-3 crops, careful comparison among crop candidates must be required. Therefore, we first model the probability of each crop being selected as the top-1 using a softmax (*i.e.*, comparison) over all crop scores:

$$\hat{p}^{\text{top1}} = \text{softmax}(\alpha[s_0, \dots, s_i, \dots, s_N]) \in \mathbb{R}^N, \quad (\text{A2})$$

where α is a scaling factor, and it is set to 2. We can view this problem as a sampling problem, where p_i^{top1} denotes the probability of sampling crop i . Selecting the best top-3 can then be formulated as sampling without replacement. The probability that crop i is selected into the top-3 is:

$$\begin{aligned} p_i^{\text{top3}} &= p_i^{\text{top1}} \\ &\quad (\rightarrow \text{crop } i \text{ is chosen first}) \\ &+ p_i^{\text{top1}} \sum_{j \neq i} \frac{p_j^{\text{top1}}}{1 - p_j^{\text{top1}}} \\ &\quad (\rightarrow \text{crop } i \text{ is chosen second}) \quad (\text{A3}) \\ &+ p_i^{\text{top1}} \sum_{j \neq i} \sum_{\substack{k \neq i \\ k \neq j}} \frac{p_j^{\text{top1}} p_k^{\text{top1}}}{(1 - p_j^{\text{top1}})(1 - p_j^{\text{top1}} - p_k^{\text{top1}})} \\ &\quad (\rightarrow \text{crop } i \text{ is chosen third}) \end{aligned}$$

This formulation is difficult to compute and optimize. Therefore, considering that there are a total of 24 crops for each image and $24 \gg 3$, we approximate the process of “sampling the top-3 without replacement” as “3 independent samplings with replacement”.

$$\hat{p}_i^{\text{top3}} = 1 - (1 - p_i^{\text{top1}})^3. \quad (\text{A4})$$

Mathematically, Eq. (A3) can be approximated by Eq. (A4) when N is large and $\max(p_i^{\text{top1}})$ is relatively small. First, in CPC, each image contains 24 crops, and $N=24$ is sufficiently larger than the sampling size of 3. Second, based on

the human-annotated p_i^{top3} , we observe that in most cases no single crop is selected among the top-3 by more than 4 out of 6 annotators, indicating that multiple crops are competitive. Thus, no crop clearly dominates others, *i.e.*, $\max(p_i^{\text{top1}})$ remains small, supporting that Eq. (A3) can be well approximated by Eq. (A4).

Loss function and optimization. We treat the composition scores s_i as learnable parameters, from which we estimate the probability that crop i is good, \hat{p}_i^{good} , and the probability that it belongs to the top-3 set, \hat{p}_i^{top3} . We define the loss as the discrepancy between the estimated probabilities and human-annotated ground truth:

$$\mathcal{L} = \sum_{i=1}^N \left((\hat{p}_i^{\text{good}} - p_i^{\text{good}})^2 + \beta (\hat{p}_i^{\text{top3}} - p_i^{\text{top3}})^2 \right), \quad (\text{A5})$$

where β is a weighting factor, and it is set to 2 by default to emphasize the top-3 term.

We optimize the scores for each original image in the CPC dataset independently. We first apply the L-BFGS [34] optimizer ($\text{lr}=1.0$, $\text{max_epochs}=10$, $\text{max_iter}=200$, $\text{history_size}=10$), which is efficient (less than 1 second per image). However, it can be unstable, leading to optimization failures. Therefore, when the final loss $\mathcal{L} > 0.5$, we switch to the Adam [22] optimizer ($\text{lr}=2e-3$, $\text{max_epochs}=5000$), which is slower (20~30 seconds per image) but more stable. Overall, the average loss converges to around 0.36. The mean absolute errors are 0.0602 between \hat{p}_i^{good} and p_i^{good} , and 0.0426 between \hat{p}_i^{top3} and p_i^{top3} , indicating sufficiently accurate probability estimation for practical use.

Post processing. The optimized composition scores are clipped and normalized to the range [1, 5] for further use.

B.2. Details of Composition Assessment Model

Composition assessment dataset collection. To train the composition assessment model, we primarily use composition scoring datasets, CADB [71] and GAIC [70], where each image is annotated with a composition score. We additionally incorporate composition classification datasets, CADB [71] and KU-PCP [25], and the aesthetic assessment dataset AVA [38], due to their strong relevance to the composition evaluation. The composition scores or aesthetic scores of each dataset are normalized to the range of [1, 5]. There are 13 composition categories in CADB dataset, *i.e.*, [center, curved, diagonal, fill the frame, golden ratio, horizontal, pattern, radial, rule of thirds, symmetric, triangle, vanishing point, vertical]. KU-PCP dataset contains 9 composition classes including [center, curved, diagonal, horizontal, pattern, rule of thirds, symmetric, triangle, vertical].

We perform data resampling strategy on the AVA and GAIC datasets to mitigate data imbalance and redundancy. First, the AVA dataset contains an excessive number of mid-quality images (*i.e.*, 97.35% in the [2,4) score range), while

Table A1. Re-sampling AVA dataset to increase the proportion of low (*i.e.*, [1,2)) and high (*i.e.*, [4,5]) score range.

Score range	[1,2)	[2,3)	[3,4)	[4,5]
Original	2,051 / 0.87%	91,401 / 38.80%	137,946 / 58.55%	4,200 / 1.78%
Re-sampled	2,051 / 4.75%	17,408 / 40.28%	19,562 / 45.26%	4,200 / 9.72%

Table A2. Statistics of our collected and re-sampled datasets to train the composition assessment model.

	Assessment			Classification	
	CADB	GAIC	AVA	CADB	KU-PCP
Train	8,547	48,140	43,221	8,547	4,244
Test	950	8,472	4,557	950	-

low-quality (*i.e.*, [1,2)) and high-quality (*i.e.*, [4,5]) samples account for only 0.87% and 1.78%, respectively, which may bias model training. Therefore, we re-sample AVA to increase the proportions of low- and high-quality images, as illustrated in Tab. A1. Second, the GAIC dataset includes 288K cropped images with MOS labels, but these are derived from only 3,336 original images, each contributing over 80 crops, resulting in insufficient data diversity. To address this, we sample 20% of GAIC, ensuring a diverse MOS distribution, which yields approximately 56K samples for training and evaluation. The final dataset statistics are summarized in Tab. A2.

Composition assessment model training using GRPO. Following Q-Insight [30] and VisualQuality-R1 [61], we adopt Qwen2.5-VL-7B [1] as the base model and train it using the GRPO [46] reinforcement learning algorithm. Specifically, for each question, we request the model to first output the thinking process in `<think></think>` tags and then output the final answer in `<answer><answer>` tags. We repeatedly request the model by N times to obtain N outputs, $\{o_1, o_2, \dots, o_N\}$. Then, for each output, we extract the answer between `<answer><answer>` tags, and calculate rewards $\{r_1, r_2, \dots, r_N\}$ by comparing the answers and ground truth. By calculating the mean and standard deviation of the rewards, the relative advantages of each response can be obtained as follows.

$$\hat{A}_i = \frac{r_i - \text{mean}(\{r_1, r_2, \dots, r_N\})}{\text{std}(\{r_1, r_2, \dots, r_N\})}, \quad (\text{A6})$$

where \hat{A}_i denotes the normalized relative advantage (quality) of the i -th response. Overall, GRPO guides the policy model to prioritize higher-quality responses that receive higher reward values within each group. After obtaining \hat{A}_i , GRPO computes the ratio between the probabilities of the same response under the updated policy $\pi_{\theta_{\text{new}}}$ and the previous policy $\pi_{\theta_{\text{old}}}$, denoted as ρ_i . To prevent excessively large policy updates and stabilize training, ρ_i is constrained within the range $[1 - \delta, 1 + \delta]$. In addition, to maintain proximity to the reference distribution π_{ref} , a KL-divergence

penalty weighted by β is introduced. Finally, the optimization objective of GRPO can be formulated as follows:

$$\begin{aligned} \mathcal{J}(\theta) = & \mathbb{E}_{q \sim \mathcal{Q}, o_i \sim \pi_{\theta_{\text{old}}}} \{ \\ & \left[\min \left(\rho_i \hat{A}_i, \text{clip}(\rho_i, 1 - \delta, 1 + \delta) \hat{A}_i \right) \right] \\ & - \beta \mathbb{D}_{\text{KL}}(\pi_{\theta_{\text{new}}} \| \pi_{\text{ref}}) \}, \end{aligned} \quad (\text{A7})$$

where $\rho_i = \pi_{\theta_{\text{new}}}(o_i | q) / \pi_{\theta_{\text{old}}}(o_i | q)$, \mathcal{Q} denotes the set of candidate questions, and \mathbb{D}_{KL} is the KL regularization term. The reference policy π_{ref} is typically a frozen pre-trained MLLM. Overall, GRPO balances consistent policy updates with strong reward signals, enabling stable yet effective optimization.

Reward calculation. To optimize Eq. (A7), we need to calculate reward r_i for each output o_i .

– *Format reward* evaluates whether the reasoning steps are properly enclosed within the `<think></think>` tags, and whether the final answer is correctly enclosed within the `<answer></answer>` tags. The format reward r_i^{format} is set to 1 if the i -th response satisfies above conditions; otherwise, it is set to 0.

– *Score reward* evaluates whether the predicted composition or aesthetic score is accurate. We first extract the model-predicted score within the `<answer></answer>` tags, then compute its error with respect to the ground-truth score. If the error is equal to or smaller than a threshold σ , the score reward r_i^{score} for the i -th response is set to 1; otherwise, it is set to 0. The threshold σ is set as 0.4 empirically.

– *Classification reward* evaluates whether the predicted composition categories match the ground-truth categories. We provide the model with all possible composition categories and ask it to select one to three of the most suitable ones (since the ground-truth annotations may contain one to three types). Let the ground truth contain n composition types, the model predict m types, and let k be the number of correctly predicted types. The classification reward is then computed as $r_i^{\text{class}} = k / \max(m, n)$.

Finally, the overall reward for the composition or aesthetic assessment task is defined as:

$$r_i = \begin{cases} r_i^{\text{format}} + r_i^{\text{score}}, & \text{if } r_i^{\text{format}} = 1, \\ 0, & \text{otherwise,} \end{cases} \quad (\text{A8})$$

and the overall reward for composition classification task is:

$$r_i = \begin{cases} r_i^{\text{format}} + r_i^{\text{class}}, & \text{if } r_i^{\text{format}} = 1, \\ 0, & \text{otherwise.} \end{cases} \quad (\text{A9})$$

With the final reward r_i for each output o_i , we then optimize Eq. (A7) to train the composition assessment model.

Implementation details. We adopt Qwen2.5-VL-7B [1] as the base model, with all model components, including



Figure A1. View-change pairs sampled by our composition assessment model from the DL3DV dataset.

the vision encoder, vision–text connector, and large language model, kept trainable. To ensure the data balance, the CADB and KU-PCP datasets are duplicated by 5 times. For each question, the number of generated responses N is set to 8. Training is performed for 1 epoch with a batch size of 32 on 8 NVIDIA A6000 GPUs using 4 gradient-accumulation steps. We employ the AdamW optimizer [19] with a learning rate of 1e-6. The coefficients β and ϵ in Eq. (A7) are set to 0.04 and 0.2, respectively.

Composition assessment results. Quantitative results of our composition assessment model have been reported in Tab. 2 of the main paper. Here, we provide additional qualitative examples in Fig. A7 and Fig. A8. The results show that our model accurately understands compositional structure and produces reliable composition scores accompanied by detailed and coherent reasoning.

B.3. Details of View-change Pairs Collection

View-change pairs sampled from the multi-view 3D dataset. We visualize the sampled View-change pairs from the DL3DV [32] dataset in Fig. A1. As shown, even the good-composition images in DL3DV reflect ordinary, casually captured viewpoints rather than expert-level compositions. This motivates the introduction of the degradation model, which is then applied to expert-taken photos to further construct higher-quality multi-view pairs.

Text–vision joint training of the degradation model. As illustrated in Fig. 11 of the main paper, incorporating text guidance leads to higher-quality results compared with image-only training. Therefore, we adopt the same text–vision joint training strategy for the degradation model. Let the good image be denoted as I_{good} , the corresponding poor image as I_{poor} , the task prompt as T_{task} , the predicted text guidance as T_{guide} , and the degradation model as $f()$. The degradation model is formulated as: $I_{\text{poor}}, T_{\text{guide}} = f(I_{\text{good}}, T_{\text{task}})$.

To train such a degradation model, we need to construct $\langle T_{\text{task}}, I_{\text{poor}}, I_{\text{good}}, T_{\text{guide}} \rangle$ samples.

The image pairs $\langle I_{\text{poor}}, I_{\text{good}} \rangle$ are collected from multi-view datasets, as illustrated in Fig. 5 of the main paper. The task prompt T_{task} , analogous to the three sub-tasks, is randomly sampled from a set of predefined template sentences such as “Change the viewpoint to *worsen* the composition”. Finally, we input each image pair into the vision language model Qwen2.5-VL-32B [1] to annotate the text guidance T_{guide} , which describes how the good image is transformed into the poor one.

With the above collected data, we could finally train the degradation model using the same text–vision joint training strategy described in Sec. 4 of the main paper. Some qualitative degradation examples generated by our degradation model are provided in Fig. A2.

Image restoration to enhance degraded outputs. As stated in the main paper, we apply the degradation model to human-taken photos produces poor-composition images. However, these degraded outputs may occasionally suffer from low visual quality with noticeable artifacts, as shown in Fig. A3. To mitigate this issue, we employ the state-of-the-art image restoration model HYPiR [31] to enhance the visual quality of degraded images. Specifically, we first down-sample each image by a factor of 4 and then use HYPiR to up-sample it by the same factor, which further suppresses generative artifacts. As illustrated in Fig. A3, HYPiR substantially improves image fidelity, yielding cleaner and more natural-looking degraded images.

B.4. Dataset Statistics

Image statistics. We have provided a rough statistic of our collected dataset in the Tab. 1 of the main paper. Here we perform a more detailed statistic of each sub-task in Tabs. A3 to A5. Since the shift and zoom-in pairs are sampled from the original images in existing cropping datasets including GAIC [70], CPC [56], SACD [64], FLMS [10], FlickrCrop [68], CUHKCrop [63], both the original images and pairs are included in the statistics. In Tab. A3, besides the collected shift pairs from GAIC and CPC, we also col-

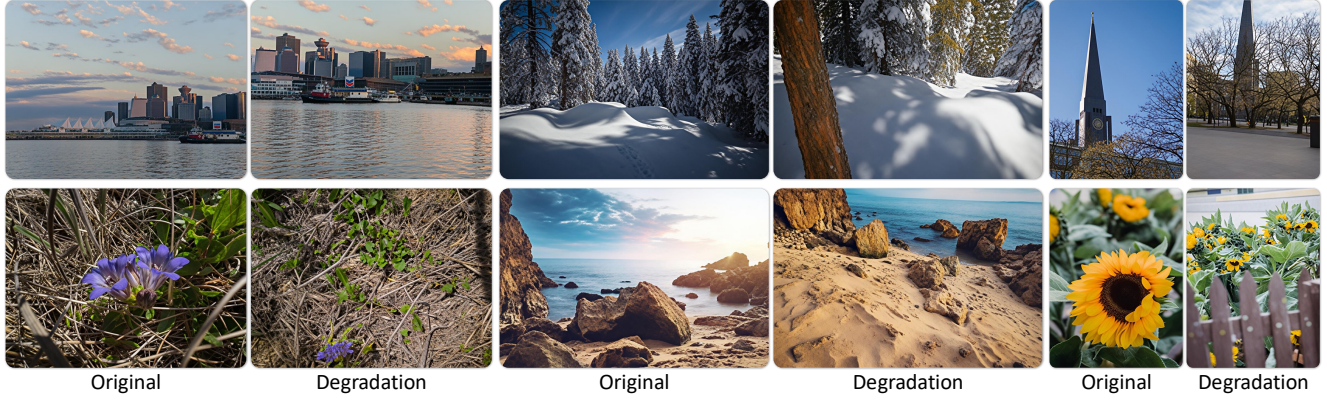


Figure A2. Degradation examples generated by our degradation model.

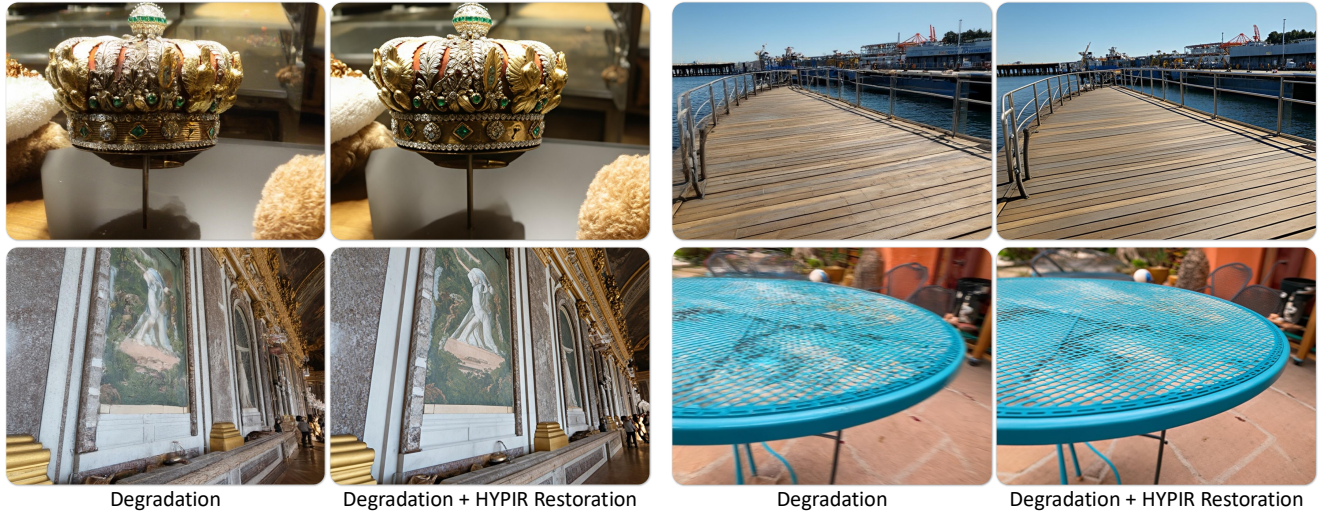


Figure A3. We use a state-of-the-art restoration model HYPiR to enhance the quality of degraded images.

Table A3. Statistics of training / test shift dataset.

	GAIC	CPC	Other
# Original	2,613 / 277	6,128 / 682	621 / -
# Pairs	72,710 / 4,578	80,486 / 6,432	698 / -

Table A4. Statistics of training / test zoom-in dataset.

	GAIC	CPC	SACD	FLMS	FlickrCrop	CUHKCrop
# Original	1,603 / 147	4,099 / 459	796 / 70	338 / -	110 / -	43 / -
# Pairs	3,830 / 327	7,426 / 869	813 / 70	686 / -	110 / -	51 / -

Table A5. Statistics of training / test view-change dataset.

	DL3DV	Unsplash Lite	Our Collected
# Pairs	13,335 / 710	7,289 / 1,000	4,340 / 719

lect a small number of shift pairs from FlickrCrop and other resources (*e.g.*, AIGC creation), denoted as “Other”.

Text statistics. We perform statistics on the text guidance length of three sub-tasks in Tab. A6. The average word

Table A6. Statistics of the text guidance length.

	Shift	Zoom-in	View-change
# Word Length	94.65	102.60	97.06
# String Length	613.43	663.16	632.77

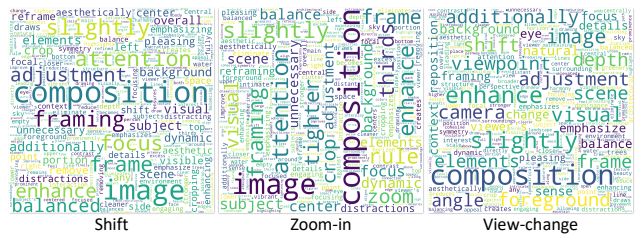


Figure A4. Word cloud of the text guidance.

length is about 100 words, providing sufficiently rich yet concise guidance for composition refinement. The word cloud of the text guidance is depicted in Fig. A4, where high-frequency words such as “composition”, “balance”, “framing”, “angle”, “viewpoint”, “tighter”, and “depth” are all closely related to compositional principles.



Figure A5. The degradation model may fail to produce a poorly composed image when given an expert-taken photo, in which case the degraded output can still appear well-composed.



Figure A6. The degradation model may alter the image excessively, leading to semantically inconsistent pairs.

B.5. Other Details

Task prompt. The task prompts for all three sub-tasks are provided in Tab. A7. Moreover, the prompts used for the two auto tasks are listed in Tab. A8.

C. Limitations and Discussions

First, the degradation model may fail to worsen the good composition. This issue is particularly common for expert-taken photos in the Unsplash Lite [9] dataset, where the degraded outputs can remain well-composed, as illustrated in Fig. A5. Fortunately, we observe empirically that including such `<good, good>` pairs does not harm the model performance. Moreover, since the users may also input such already well-composed images, we intentionally retain these samples rather than filtering them out.

Second, the degradation model may change the image excessively, producing pairs that are no longer semantically consistent. As shown in Fig. A6, the degraded output deviates notably from the original content. Although we perform data filtering, a small number of such inconsistent pairs may still remain. Future work should explore a more controllable degradation model to reduce inconsistency.

Third, the generated images may exhibit relatively low

visual quality, as depicted in Fig. A3. However, image quality is not the primary focus of our work, and we are concerned chiefly with composition. Improving the quality of generated images can be explored in our future work.

Fourth, we emphasize that synthetic data provides only an initial foundation for training composition instruction models. While it enables large-scale supervision and controlled variation, it cannot fully replace real-world images captured by everyday mobile users, which exhibit diverse shooting habits, device characteristics, and natural composition errors. Constructing such a real, human-captured dataset will be crucial for advancing composition instruction and remains an important direction for future work.

Table A7. **Task prompt** of three sub-tasks.

#	Shift Prompt
1	Shift the framing of this scene to improve its overall composition.
2	Shift the camera to make the scene more visually appealing.
3	Adjust the framing by shifting to create a stronger composition.
4	Reframe by shifting to enhance the visual composition.
5	Shift the view to improve the image composition.
6	Reframe by shifting to make the scene more pleasing.
7	Refine the image composition by shifting the frame.
8	Shift the scene to enhance the composition.
9	Enhance the scene by shifting the camera framing.
10	Shift the frame to create a stronger composition.

#	Zoom-in Prompt
1	Zoom in the framing of this scene to improve its overall composition.
2	Tighten the framing by zooming in to make the image more appealing.
3	Zoom in to refine the composition and enhance the visual effect.
4	Narrow the framing by zooming in for a more pleasing result.
5	Adjust the composition by zooming in to strengthen the image.
6	Reframe by zooming in to make the scene look more polished.
7	Refine the composition by zooming in to simplify the frame.
8	Enhance the image by narrowing the view with a zoom-in.
9	Strengthen the composition by zooming in.
10	Make the image look cleaner by zooming in on the framing.

#	View Change Prompt
1	Change the viewpoint of this scene to improve its overall composition.
2	Make a view change to find a better shooting point and improve the composition.
3	Perform a view change to choose a more appealing shooting spot.
4	Select a new shooting view to create a better composition.
5	Change the shooting view to achieve a more visually pleasing shooting point.
6	Explore a different shooting spot to improve the overall composition.
7	Change the shooting view to create a more effective composition.
8	Make a view change to enhance the composition of the scene framing.
9	Apply a view change for a more engaging and visually strong composition.
10	Change the viewpoint to make the composition more attractive.

Table A8. **Task prompt** of two auto tasks.

#	Prompt for Static Auto Task (Shift or Zoom-in)
1	Refine the composition through shift or zoom-in adjustments.
2	Improve the composition by combining shift or zoom-in operations.
3	Enhance the image composition with coordinated shift or zoom-in refinement.
4	Adjust the framing through shift or zoom-in to achieve a better composition.
5	Make the composition more appealing using shift or zoom-in adjustments.
6	Refine the scene composition with gentle shift or zoom-in movement.
7	Improve the framing by applying continuous shift or zoom-in optimization.
8	Enhance the overall composition through integrated shift or zoom-in refinement.
9	Adjust the frame smoothly using shift or zoom-in to strengthen composition.
10	Refine the image framing through natural shift or zoom-in enhancement.

#	Prompt for Full Auto Task (All Three Tasks)
1	Capture this scene with better composition.
2	Enhance the composition of this scene.
3	Refine the composition to make this scene more visually pleasing.
4	Adjust the image to improve its composition.
5	Reframe this scene to achieve a more pleasing visual composition.
6	Refine the framing through shift, zoom-in, or view change.
7	Improve the composition through shift, zoom-in, or viewpoint adjustment.
8	Enhance the image composition through shift, zoom-in, and view change.
9	Optimize the composition through shift, zoom-in, or new viewpoint exploration.
10	Refine the scene composition through shift, zoom-in, or view change as needed.

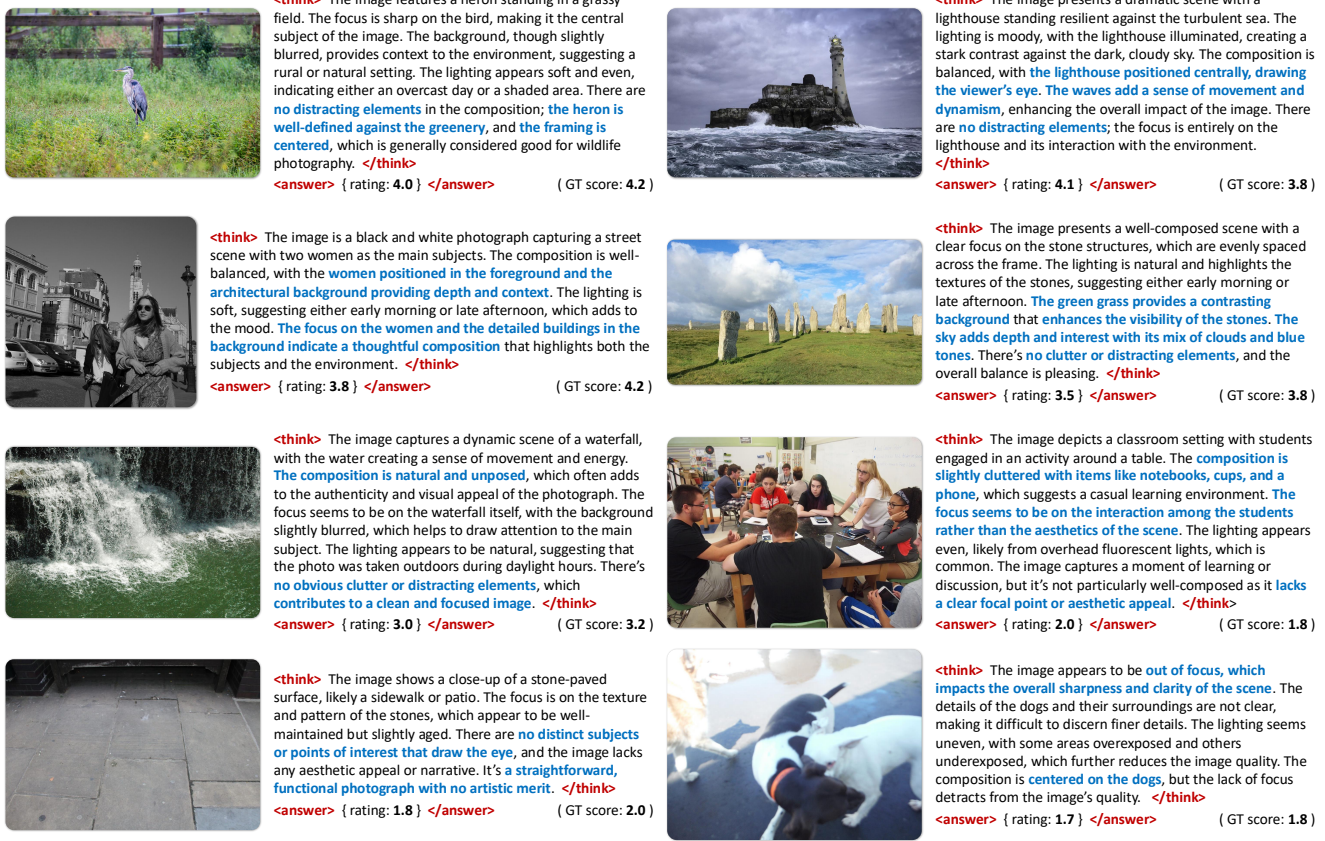


Figure A7. Qualitative results of image composition assessment on CADB dataset.

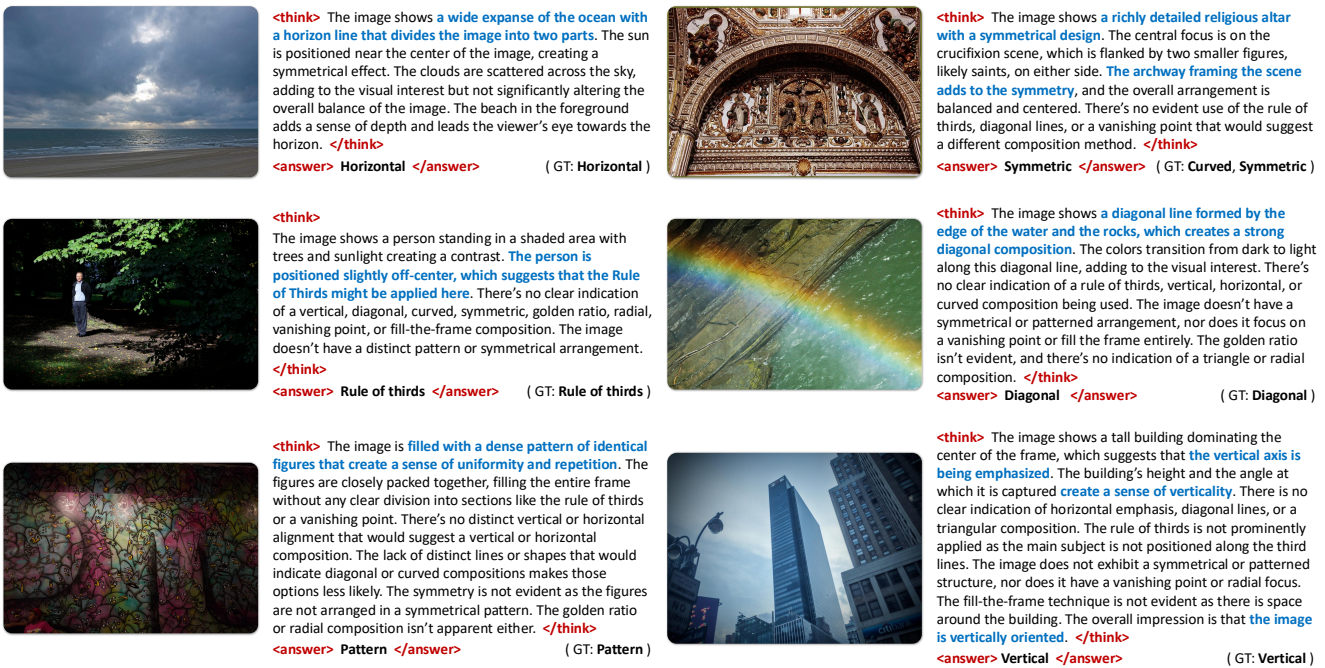


Figure A8. Qualitative results of image composition classification on CADB dataset.



To enhance the composition, adjust the framing by **cropping out the lower portion of the field, focusing on the upper half where the white structure stands prominently against the tree line**. This change emphasizes the contrast between the bright field and the darker trees, creating a stronger visual hierarchy. Additionally, **include more of the sky above the trees** to introduce a sense of openness and balance the vertical elements. This modification draws attention to the structure as the central subject, while the remaining greenery provides a natural frame, improving overall harmony and aesthetic appeal.



To enhance the composition, crop the image to **focus on the person in the red coat as the central subject**, placing them slightly off-center to adhere to the rule of thirds. **Remove the top portion of the image where the sky dominates**, as it currently draws attention away from the main subject. **Adjust the bottom edge to include more of the snowy path leading into the distance**, creating a stronger leading line that guides the viewer's eye through the scene. This modification will emphasize the subject while maintaining the rural winter setting, improving overall balance and visual flow.



To enhance the composition, adjust the framing by **cropping out the lower portion of the image, focusing on the upper half where the silhouette of the boat and the sunset are more prominent**. This change eliminates unnecessary water surface details, creating a cleaner and more balanced visual weight. By **centering the boat horizontally and aligning it with the reflection of the sun**, the composition becomes more symmetrical and aesthetically pleasing. The reduced water area draws attention to the warm hues of the sunset and the silhouette, emphasizing the serene and tranquil mood of the scene. This modification ensures the viewer's focus remains on the key elements without distraction.



To enhance the composition, **crop the image slightly closer to the subjects' faces**, ensuring they are **centered and more prominent**. Remove any unnecessary background elements that distract from the focus on the individuals. **Adjust the framing so that the lights in the background create a soft bokeh effect**, adding depth without overpowering the subjects. This tighter crop will emphasize their expressions and attire, making them the clear focal point while maintaining a balanced and aesthetically pleasing composition.



To enhance the composition, crop the image to **focus on the central area where the tram tracks lead into the frame**, creating a strong leading line that draws the viewer's eye deeper into the scene. **Remove the lower portion of the snowy sidewalk**, which appears less dynamic and reduces visual clutter. **Adjust the framing to include more of the illuminated building and its festive decorations**, such as **the "Cafe" sign** and the Christmas tree, to emphasize the warm, inviting atmosphere. This shift balances the composition by highlighting the architectural details and the activity around them, making the scene feel more vibrant and engaging.



To enhance the composition, adjust the framing by **centering both dogs more prominently in the scene**. Ensure they are **fully visible**, with their entire bodies including their heads and legs, to emphasize their playful energy. **Remove any distracting elements on the left side**, such as **the partial view of the dog**, to create a cleaner focus on the two main subjects. Additionally, slightly increase the depth of field to **keep the background softly blurred**, ensuring the dogs remain the focal point. This adjustment balances the composition, highlights the dynamic movement of the dogs, and creates a more engaging and aesthetically pleasing image.



To enhance the composition, **crop the image to focus on the colorful birdhouse and its reflection in the water**, placing them closer to the center. **Remove the distracting empty branches on the left side** to create a cleaner frame. Adjust the background by reducing the visible area of the bridge and distant trees, emphasizing the serene water and the birdhouse as the primary subjects. This shift draws attention to the vibrant colors and reflections, creating a more balanced and aesthetically pleasing image. The tighter framing also eliminates unnecessary elements, making the scene feel more intimate and focused.



To enhance the composition, crop the image slightly **closer to the lighthouse and house, focusing on their structures and the rocky foreground**. Remove the excess empty space **above the clouds** to emphasize the dramatic sky and create a stronger visual connection between the elements. This adjustment draws attention to the lighthouse as the central subject, while the house adds depth and context. The tighter framing also balances the weight of the sky and sea, making the overall scene more dynamic and visually engaging.



To enhance the composition of the original image, adjust the framing by **lowering the horizon line to include more of the foreground**, such as **the road and any visible structures or vegetation**. This change will create a stronger sense of depth and context, grounding the majestic mountains in their environment. Additionally, **ensure that the road leads the viewer's eye towards the mountains**, using the natural lines of the landscape to guide attention. This modification balances the vastness of the sky with the earthy tones of the foreground, making the overall scene more dynamic and engaging.



To enhance the composition of the original image, reframe it by **centering the butterfly more prominently** within the frame. This adjustment ensures the butterfly is the clear focal point, drawing attention to its intricate wing patterns and delicate details. Additionally, **crop out any unnecessary grass blades on the left side** to eliminate distractions and create a cleaner, more balanced composition. By doing so, the greenery serves as a soft, natural backdrop that complements the butterfly without overpowering it, resulting in a more aesthetically pleasing and focused image.

Figure A9. Qualitative results of the shift task. Left / right / bottom: original image / generated example image / text guidance. Actionable textual suggestions are highlighted in **blue**, while hallucinated descriptions are marked in **red**.



To enhance the composition, **zoom in on the skier**, centering them more prominently. **Remove the top portion with the banner and people in the background** to minimize distractions. **Position the skier slightly off-center** to follow the rule of thirds. This tighter framing focuses attention on the skier's action and the snowy slope, creating a dynamic and engaging image.



To improve the composition, **zoom in closer to the woman, focusing on her face and upper body** while **excluding the laptop and knitting materials**. This shift centers attention on her expression and interaction with the knitting needles, creating a more intimate and engaging scene. By removing the laptop, you eliminate distractions and emphasize the personal, creative activity. Adjust the framing to **place her slightly off-center**, following the rule of thirds, which adds visual interest and balance. This tighter crop also simplifies the background, drawing the viewer's eye to her actions and emotions.



To enhance the composition, **zoom in on the subject by cropping out the lower portion** of the image, focusing on the man from just above his waist up. This adjustment **eliminates unnecessary ground space**, creating a more dynamic and centered composition. By keeping the subject slightly off-center (to the left), you adhere to the **rule of thirds**, adding visual interest. The tight framing also removes extraneous details in the background, such as the lower part of the building and the floor, which helps draw attention to the subject's gesture and expression. The vibrant purple lighting behind him remains prominent but is now framed more intentionally, enhancing the overall aesthetic balance and focus.



To improve the composition, **zoom in and crop the scene to focus more tightly on the cat and the ornate green bench**. **Eliminate the excess yellow wall space above and below the bench**, which currently dominates the frame. By reframing, the cat becomes the central subject, drawing immediate attention due to its position and the contrast against the vibrant green background. This tighter crop also accentuates the intricate details of the bench's design, creating a more dynamic and engaging visual. Additionally, removing the empty space around the edges reduces distractions and emphasizes the harmony between the cat and its environment, adhering to the rule of thirds for a balanced and aesthetically pleasing result.



To enhance the composition, **zoom in slightly to center the train more prominently**. This adjustment **reduces empty space on the sides, focusing attention on the train and its lights**. Position the train off-center following the rule of thirds for a balanced look. Eliminate distractions like distant poles and shrubs to emphasize the train and the mountainous backdrop, creating a clearer, more engaging image.



To enhance the composition, **zoom in on the surfer and wave, removing the top-left tree branches and bottom-right observer**. This tight framing focuses attention on the surfer's action and the wave's texture. **Centering the surfer within the wave** adheres to the rule of thirds, creating balance. Eliminating distractions sharpens the viewer's focus, resulting in a more dynamic and engaging image.



To enhance the composition of the image, **zoom in and reframe to focus on the bus as the central subject, eliminating unnecessary foreground elements like the person walking and the parked cars** on the left. This adjustment reduces distractions and directs attention to the bus's vibrant colors and movement. **Shift the framing slightly to place the bus near the center** but not perfectly aligned, adhering to the rule of thirds for a more dynamic feel. By removing the lower portion of the image, including the road markings and some vehicles, the composition becomes cleaner and more focused, emphasizing the bus's journey against the backdrop of the large building and flags. This reframing creates a stronger visual narrative and balance.



To enhance the composition, **zoom in on the tennis player**, centering him more prominently. This **eliminates excess background and focuses attention on his action**. Adjust the angle slightly to align him with the court lines, **adhering to the rule of thirds**. This tighter framing creates a dynamic, engaging image that emphasizes the athlete's movement and the vibrant court colors.



To enhance the composition of the image, **zoom in and reframe to focus on the narrow gauge train as the central subject, eliminating unnecessary foreground elements like the road and the distant house**. This adjustment brings attention to the train's details and its interaction with the landscape, such as the vibrant orange flowers and rolling hills. By placing the train slightly off-center, following the rule of thirds, the composition becomes more dynamic and balanced. The tighter frame also reduces distractions from peripheral elements, emphasizing the harmony between the train and the scenic backdrop, creating a more cohesive and aesthetically pleasing image.



To enhance the composition, **zoom in and reframe to focus on the lighthouse and its immediate surroundings**. **Crop out the top portion of the sky**, which is mostly empty and does not add significant visual interest. **Shift the framing slightly to bring the lighthouse and rocky outcrop closer to the center**, emphasizing their prominence. Reduce the visible expanse of the ocean on the left side to create a more balanced and intimate view. This reframing brings attention to the interplay between the natural landscape and the man-made structure, enhancing the aesthetic by creating a more dynamic and focused scene.

Figure A10. Qualitative results of the zoom-in task. Left / right / bottom: original image / generated example image / text guidance. Actionable textual suggestions are highlighted in **blue**, while hallucinated descriptions are marked in **red**.



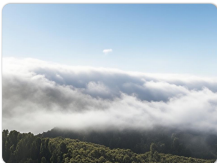
To enhance the composition, adjust the viewpoint to **emphasize the expansive coastal landscape while reducing the prominence of the dry, thorny foreground vegetation**. Shift focus slightly upward to reveal more of the serene ocean horizon and the distant coastline, creating a sense of depth and vastness. **Crop out some of the distracting, dense vegetation in the lower portion**, allowing the natural beauty of the flowers and the open sky to take center stage. This change balances the elements, highlighting the contrast between the rugged terrain and the tranquil sea, resulting in a more harmonious and aesthetically pleasing image.



To enhance the composition, **zoom in on the sunflower and crop out the background elements such as the road, trees, and distant structures**. This **focuses attention on the flower and its immediate surroundings**, creating a more intimate and striking visual. By **removing distractions like the empty parking lot and utility poles**, the viewer's gaze is drawn directly to the vibrant yellow sunflower, which becomes the central point of interest. Additionally, this closer framing emphasizes the contrast between the delicate flower and the rough texture of the surrounding rocks, enhancing the overall aesthetic appeal and emotional impact.



To enhance the composition, reposition the viewpoint to **include more of the expansive ocean and distant horizon**, creating a sense of scale and depth. Shift focus slightly upward to minimize the dominance of the sandy foreground and emphasize the rugged textures of the cliffs. **Incorporate more sky to balance the heavy rock formations and add visual interest with clouds or clear blue tones**. This adjustment will draw the viewer's eye across the scene, from the detailed cliff textures to the vastness of the sea and horizon, resulting in a more dynamic and aesthetically pleasing image.



To enhance the composition, adjust the viewpoint to **focus on the dramatic interplay between the clouds and the landscape**. Place the horizon line higher in the frame to emphasize the expansive sky and cloud cover, creating a sense of grandeur and scale. **Remove the signpost from the right side to eliminate distractions** and allow the natural elements to take center stage. **Shift slightly to include more of the tree line at the edge of the cloud layer**, which will add depth and visual interest. This change directs attention to the contrast between the earthy tones below and the ethereal quality of the clouds above, resulting in a more balanced and aesthetically pleasing image.



To enhance the composition, reposition the viewpoint to **focus solely on the urban skyline at night, eliminating the foreground vegetation and pole**. This simplifies the scene, allowing the illuminated buildings to become the central visual element. By **removing distractions such as the natural elements and the pole**, the viewer's attention is drawn directly to the architectural details and the interplay of light and shadow. The resulting image will emphasize symmetry, depth, and the vibrant cityscape, creating a more cohesive and aesthetically pleasing photograph.



To enhance the composition, adjust the viewpoint to **focus more on the vibrant yellow trees**, ensuring they occupy a larger portion of the frame. **Crop out the lower foreground rocks and dirt path** to minimize distractions and emphasize the verticality of the trees. **Shift the horizon line slightly higher to include more of the clear blue sky**, which will balance the warm tones of the foliage and add depth. This change will highlight the contrast between the golden trees and the cool sky, creating a more striking and aesthetically pleasing image.



To enhance the composition, adjust the viewpoint to **place the dome of the building more centrally and prominently** within the frame, ensuring it becomes the focal point. **Remove the foreground trees that partially obscure the structure**, allowing the full grandeur of the architecture to be appreciated. **Shift the angle slightly upward to emphasize the height and symmetry of the building against the clear blue sky**. This change will create a more balanced and aesthetically pleasing image, highlighting the historical and architectural significance of the scene. Additionally, consider reducing distractions such as the yellow structure on the right side to maintain visual harmony.



To enhance the composition, adjust the viewpoint by **focusing on a single prominent leaf in the foreground**, creating a clear point of interest. **Shift the perspective slightly upward to minimize the dominance of the asphalt surface** and emphasize the scattered leaves and their natural patterns. **Include more of the background trees and foliage to add depth and context**, ensuring the sun's glow is visible through the leaves to introduce warmth and contrast. This change directs the viewer's gaze naturally along the path, enhancing the sense of movement and seasonal ambiance.



To enhance the composition, adjust the viewpoint to **focus more on the expansive green field and the distant cityscape**, creating a stronger sense of depth and scale. Place the horizon line **higher** in the frame to **emphasize the vastness of the open space and the urban skyline beyond**. **Remove distractions such as the fence and people near the bottom**, allowing the viewer's eye to flow freely across the field. Incorporate more of the palm trees and surrounding buildings to add texture and context without overcrowding the scene. This shift will balance the natural and urban elements, highlighting the contrast between the serene park and the bustling city.



To enhance the composition, **focus solely on the palm tree and rainbow**, removing the building from the frame. **Place the tree centrally** to emphasize its natural elegance and allow the rainbow to arc gracefully across the clear sky, creating a strong visual contrast. **Eliminate distractions such as the balcony and roofline**, which currently compete for attention. This adjustment will highlight the serene beauty of the scene, balancing the vibrant colors of the rainbow against the lush green foliage and the soft blue sky. The result will be a more harmonious and aesthetically pleasing image that draws the viewer's eye naturally to the interplay between nature's elements.

Figure A11. Qualitative results of the view-change task. Left / right / bottom: original image / generated example image / text guidance. Actionable textual suggestions are highlighted in **blue**, while hallucinated descriptions are marked in **red**.